

The RavA-ViaA Chaperone-Like System Interacts with and Modulates the Activity of the Fumarate Reductase Respiratory Complex

Keith S. Wong^{1,*}, Vaibhav Bhandari^{1,*}, Sarath C. Janga², and Walid A. Houry^{1,3,#}

¹Department of Biochemistry, University of Toronto, Toronto, Ontario M5G 1M1, Canada

²Department of Biohealth Informatics, School of Informatics and Computing, Indiana University Purdue University, Indianapolis, Indiana 46202, USA.

³Department of Chemistry, University of Toronto, Toronto, Ontario M5S 3H6, Canada

*These authors contributed equally to this work.

#To whom correspondence should be addressed:

Walid A. Houry
Department of Biochemistry
Faculty of Medicine
University of Toronto
MaRS Centre, West Tower
661 University Ave., Suite 1600
Toronto, ON M5G 1M1
CANADA
Phone: (416) 946-7141
FAX: (416) 978-8548
Email: walid.houry@utoronto.ca

Running title: RavA-ViaA interact with the fumarate reductase complex

Keywords: ATPases associated with diverse cellular activities (AAA); Chaperone; Flavoprotein; Respiratory chain; von Willebrand factor A domain

ACCEPTED MANUSCRIPT

Highlights

1. RavA-ViaA form a chaperone-like complex interacting with respiratory chains.
2. RavA-ViaA are induced under oxygen-limiting conditions.
3. RavA-ViaA interact with the flavin-containing subunit of fumarate reductase.
4. RavA-ViaA modulate the activity of the fumarate reductase complex.

Abstract

RavA is a MoxR AAA+ protein that functions together with a partner protein that we termed ViaA containing a von Willebrand Factor A (VWA) domain. However, the functional role of RavA-ViaA in the cell is not yet well-established. Here, we show that RavA-ViaA are functionally associated with anaerobic respiration in *Escherichia coli* through interactions with the fumarate reductase (Frd) electron transport complex. Expression analysis of *ravA* and *viaA* genes showed that both proteins are co-expressed with multiple anaerobic respiratory genes, many of which are regulated by the anaerobic transcriptional regulator Fnr. Consistently, the expression of both *ravA* and *viaA* was found to be dependent on Fnr in cells grown under oxygen-limiting condition. ViaA was found to physically interact with FrdA; the flavin-containing subunit of the Frd complex. Both RavA and the Fe-S-containing subunit of the Frd complex, FrdB, regulate this interaction. Importantly, Frd activity was observed to increase in the absence of RavA and ViaA. This indicates that RavA and ViaA modulate the activity of the Frd complex, signifying a potential regulatory chaperone-like function for RavA-ViaA during bacterial anaerobic respiration with fumarate as the terminal electron acceptor.

[187 words]

Introduction

The MoxR family of AAA+ ATPases is relatively unknown, although it is diverse and widespread among bacteria and archaea [1]. The experimental evidence gathered on various MoxR proteins suggests that they have regulatory and chaperone-like roles in the maturation of protein complexes participating in a variety of biological processes including metabolism, cell morphology and development, tolerance against various types of stress, and pathogenesis [1-4]. A characteristic of the MoxR AAA+ ATPases is that their genes co-occur in close proximity with one or more genes whose proteins contain the von Willebrand factor A (VWA) domain [1]. The VWA domain features the conserved MIDAS (Metal Ion-Dependent Adhesion Site) motif, which binds a single divalent cation, usually Mg^{2+} , and mediates protein-protein interactions [5].

The functional characterization of the MoxR protein RavA (Regulatory ATPase variant A) and its corresponding VWA protein ViaA (VWA interacting with AAA+ ATPase) in *Escherichia coli* is an ongoing effort in our laboratory. RavA belongs to the eponymous RavA subfamily of the MoxR family [1]. The *ravA* and *viaA* genes are organized in a pattern that is typical of this subfamily with *ravA* positioned immediately upstream of *viaA* and with both genes forming a single operon [6]. In aerobically grown cells, the *ravAviaA* operon is induced by the stationary phase sigma factor, σ^S [6]. RavA has been characterized extensively by our group both biochemically and biophysically. It forms a hexameric complex [6, 7], which is typical for most AAA+ ATPases [8]. *In vitro*, the ATPase activity of RavA is optimal at neutral pH and 37 °C, which is enhanced in the presence of ViaA [6]. In stationary phase cells, RavA was found to mainly localize to the cytoplasm, while ViaA was found to be localized to both the cytoplasm and the inner membrane [9].

Although little is known about their cellular function, several interaction partners for

RavA have been identified that suggest its involvement in potential regulatory roles in different biological processes. For example, RavA associates with and modulates the activity of the inducible lysine decarboxylase (LdcI) [6, 7, 10, 11], a major acid stress response protein in *E. coli* [10, 12]. The alarmone, ppGpp, was found to bind and inhibit the activity of LdcI, and the interaction of RavA with LdcI prevented this binding of ppGpp to LdcI [7]. This supports a potential role of RavA, and possibly ViaA, in bacterial acid stress response [7]. In addition, RavA and ViaA were functionally linked with bacterial respiration when they were shown to sensitize the cell to aminoglycosides [9, 13]. The identification of null mutations that suppressed this phenotype, and subsequent immunoprecipitation experiments, revealed that RavA and ViaA interact with specific subunits of the NADH:ubiquinone oxidoreductase I (Nuo complex) [9]. The Nuo complex, commonly known as Complex I, is a major player in the aerobic respiration of *E. coli* [14, 15]. It is also important in anaerobic respiration utilizing fumarate and dimethylsulfoxide [16].

High-throughput studies have revealed functional links between RavA-ViaA with several pathways that are directly or indirectly related to bacterial respiration. These include iron-sulfur (Fe-S) cluster biosynthesis, iron transport, and anaerobic electron transport [9, 17]. In this study, we present evidence that supports a regulatory role of the RavA-ViaA proteins in the activity of the anaerobic respiratory complex fumarate reductase (Frd). The *E. coli* fumarate reductase complex catalyzes the final step of anaerobic respiration when fumarate acts as the terminal electron acceptor [18]. The complex is formed by four subunits (FrdABCD) [19, 20] with FrdC and FrdD being the membrane-spanning subunits, while the flavoprotein FrdA and the iron-sulfur cluster-containing protein FrdB comprising the soluble part of the complex. During anaerobic respiration, menaquinol (MQH₂) in the membrane donates electrons to the fumarate

reductase complex [21]. The membrane spanning FrdCD subcomplex anchors the FrdAB components to the membrane and, along with FrdB, provide binding sites for the quinones. The electrons then traverse through the three iron-sulfur clusters present in FrdB to the FAD cofactor in the FrdA active site where they are used to reduce fumarate to succinate [20-23]. Here, we find ViaA to interact with free FrdA through its C-terminal VWA domain and with RavA through its N-terminal α -helical rich domain. Importantly, the interaction of RavA-ViaA with FrdA results in a decrease in Frd activity. A model of the effect of RavA-ViaA on the maturation of the Frd complex is proposed.

Results

***ravA* and *viaA* display similar co-expression profiles as those of the Fnr-inducible genes**

We had earlier demonstrated that RavA-ViaA interact with LdcI and the Nuo complex [2, 6, 9]. However, given that we postulated that RavA-ViaA might have chaperone-like activity [1, 2], further studies were carried out to identify new interacting partners for this system. Initially, co-expression profiling was performed to identify genes that co-express with both *ravA* and *viaA*. This approach is based on the principle that genes are organized in a network of distinct, functional modules or hubs with highly coordinated expression patterns that correspond to specific biological processes [24-27]. Thus, genes that are functionally associated have a higher likelihood of sharing common transcriptional regulatory elements and of displaying similar expression profiles in response to the same physiological signals or external environmental stimuli.

The co-expression profiles for *ravA* and *viaA* genes were constructed by data-mining a public collection of 445 *E. coli* microarray datasets collected across multiple experimental

conditions, and then genes that displayed highly similar co-expression patterns with *ravA* and *viaA* were identified. Our analysis yielded a total of 62 genes that co-express with *ravA* and 56 that co-express with *viaA* (Fig. 1A; Table 1). Of these, 32 genes co-express with both *ravA* and *viaA*. Given that *ravA* and *viaA* are in the same operon [1, 6], genes that are co-expressed with both *ravA* and *viaA* were considered as the most reliable candidates for functional association and were examined further.

One important trend uncovered in our analysis is that many of the genes that co-express with both *ravA* and *viaA* are involved in anaerobic respiration. These include *frdA*, *frdB*, and *frdC*, which encode three of the four subunits of the fumarate reductase complex (FrdABCD); *nirB* and *nirD*, which encode the large and small subunits, respectively, of the nitrite reductase complex (NirDB₂); *hybO*, which encodes the small subunit of hydrogenase 2 (HybABOC); and *nrfA*, which is the structural gene for cytochrome *c*₅₅₂ and a component of the formate-dependent nitrite reductase complex (NrfDCBA).

A second group of genes falls under protein maturation and modification, all of which – *hypA*, *hypB*, *hypC* and *hypD* – are involved in the insertion of Ni²⁺ ion for the maturation of the membrane-bound hydrogenase 3 (HycDCFGBE), and, thus, are also associated with anaerobiosis. Hydrogenase 3 works in conjunction with formate dehydrogenase H (FdhF) in both mixed acid fermentation and anaerobic respiration. Other genes that co-express with both *ravA* and *viaA* participate in various metabolic pathways (*gpmM*, *mtlD*, *pfkA*, *ansB*, *aspA*, *selA*, *pepE*, *pldB*, and *udp*), biosynthesis of cofactors and prosthetic groups (*hemC*, *hemX*, and *menD*), and transport of metabolites across the cell membrane (*dcuA*, *dcuB*, and *nikA*).

Importantly, 14 out of the 32 genes that co-express with *ravA* and *viaA* are inducible by the transcriptional regulator Fnr (marked with * in Fig. 1A). In *E. coli*, Fnr regulates the

expression of a large number of genes during the transition from aerobiosis to anaerobiosis [28, 29]. The co-expression of genes under Fnr control suggested that Fnr was also likely to regulate the expression of both *ravA* and *viaA*.

Fnr enhances the expression of RavA and ViaA during oxygen-limiting conditions

To determine whether the expression of RavA and ViaA was indeed regulated by Fnr, WT along with the null mutants $\Delta fnr::kan^R$ and $\Delta rpoS::kan^R$ were grown in liquid media under aerobic or oxygen-limiting conditions. Cell growth was monitored by measuring OD₆₀₀ at specific time points. When cells were grown aerobically, all three strains shared almost identical growth profiles (Fig. S1). On the other hand, during oxygen-limiting growth, $\Delta fnr::kan^R$ exhibited a minor growth lag from early log to late log phase, and both $\Delta fnr::kan^R$ and $\Delta rpoS::kan^R$ had only a slightly lower cell count per unit volume compared to WT upon reaching stationary phase (Fig. S1). These relatively small differences in growth between WT and the two mutants helped to minimize changes in experimental protocol, which were made to accommodate their different growth profiles.

The expression levels of RavA and ViaA in each strain were then analyzed by Western blotting. Under aerobic condition, WT cells displayed the expected RavA expression profile as reported previously [6], with minimal expression during log phase that increases to optimum at stationary phase (Fig. 1B). Interestingly, under oxygen-limiting condition, RavA expression was significantly enhanced in WT cells at all growth phases, which indicates that oxygen starvation is likely an important inducer of RavA protein expression. Importantly, unlike in the WT cell line, the expression of RavA in $\Delta fnr::kan^R$ cells did not increase during oxygen-limiting growth. Thus, Fnr was deemed necessary for the enhanced expression of RavA when oxygen is limiting.

Furthermore, as previously reported in aerobically grown $\Delta rpoS::kan^R$ cells, the expression of RavA was severely compromised due to the loss of σ^S [6]. In contrast, under oxygen-limiting condition, the expression of RavA in $\Delta rpoS::kan^R$ closely resembles that of WT, although the further increase in RavA levels after 6 hours observed in WT was not observed in $\Delta rpoS::kan^R$ (Fig. 1B). This strongly supports the conclusion that the expression of RavA during oxygen starvation is largely dependent on Fnr and not σ^S , but σ^S might have some role at later time points.

Like RavA, the expression of ViaA shows a similar dependence on Fnr in cells during oxygen starvation. In WT cells, ViaA expression was significantly enhanced and the deletion of σ^S did not affect this enhancement; however, in the absence of Fnr, no such enhancement was observed (Fig. 1B). It is interesting to note that ViaA expression during oxygen-limiting growth was higher in log phase compared to stationary phase – the reverse of RavA. This was most apparent in WT and $\Delta fnr::kan^R$ cells (Fig. 1B). In contrast, ViaA expression was largely unchanged in $\Delta rpoS::kan^R$ cells during oxygen starvation from log phase to stationary phase (Fig. 1B). Since both *ravA* and *viaA* are on the same operon [6] and there is no recognizable promoter upstream of *viaA*, the difference in the expression profiles of RavA and ViaA likely reflects the presence of additional regulatory elements affecting either mRNA or protein levels that are dependent on σ^S .

Overall, our results clearly illustrate that, under oxygen-limiting conditions, Fnr functionally replaces σ^S and becomes the primary regulator for the expression of both RavA and ViaA, which makes both the *ravA* and *viaA* genes novel constituents of the Fnr regulon. However, σ^S continues to play a role in RavA and ViaA expression under these conditions.

Identification of potential Fnr-binding sites in the native promoter region of *ravAviaA*

The Fnr-induced expression of *RavA* and *ViaA* cells during oxygen-limiting growth indicates the existence of regulatory elements in the *ravAviaA* promoter region for Fnr binding. Identification of such elements would further validate the results of Figure 1.

Using knowledge-based sequence motifs recognition software such as Virtual Footprint [30], SCOPE [31] and PromoScan [32], our initial analysis of the genomic sequence of this region to identify potential binding sites of various transcriptional regulators revealed two potential Fnr binding sites: one centered at -72.5 (**TTAACCTGGCTCAA**; bolded bases represent perfect matches to the Fnr consensus sequence) and another one located further upstream at -188.5 (**TTGCTTATTATCAG**) (Fig. 2A,B). Both sites are similar to the Fnr consensus sequence TTGATnnnnATCAA (n represents any base) [33], but they lack the characteristic palindromic sequences that flank the two ends.

To further examine these two potential binding sites for Fnr, three linear DNA substrates of the same length but encompassing different parts of the *ravAviaA* promoter region (R-1, R-2 and R-3; Fig. 2C) were synthesized by PCR for use in EMSA assays with Fnr_{D154A}. The Fnr_{D154A} mutant, which has the same affinity and specificity for the Fnr consensus sequence as its WT counterpart [34], was used so that the EMSA experiments could be performed under aerobic conditions. As shown in Fig. 2D, the inclusion of Fnr_{D154A} in the sample induced significant band shifts for DNA substrates R-1 (which has both the -72.5 and -188.5 Fnr binding sites) and R-2 (which retains only the -72.5 site). In contrast, band shift was reduced for substrate R-3, which lacks both supposed Fnr binding sites. As both R-1 and R-2 displayed very similar band shifts in the presence of Fnr_{D154A}, the -188.5 site did not appear to be necessary for binding. In other words, the interaction between Fnr_{D154A} and the *ravAviaA* promoter appears to be largely

mediated through the -72.5 site.

To provide additional proof that the interaction between Fnr_{D154A} and the DNA substrates R-1 and R-2 was specific, EMSA was repeated using the following substrates: F-1 as negative control and H-1, H-2 and H-3 as positive controls (Fig. 2E-G). Substrate F-1 encompasses the entire *fepDGC* promoter region, which carries four binding sites for the Fe²⁺-sensing Fur [35-37] but none for Fnr. Substrate H-1 encompasses the *hypBCDE* promoter region that is internal to the *hypA* gene. It contains two Fnr binding sites – one centered at -43.5 (**TTGATCTGGTTTGC**; bolded bases represent perfect matches to the Fnr consensus sequence) and the other one further upstream at -149.5 (**TTGATCGAACAGCA**) [38]. Following the same scheme used in examining the Fnr binding sites from the *ravAviaA* promoter, substrates H-2 (only the -43.5 site is retained) and H-3 (all Fnr binding sites removed) were also synthesized. As shown in Fig. 2G, Fnr_{D154A} did not interact with either F-1 or H-3, as neither substrate carries Fnr binding sites. On the other hand, H-1 contains both Fnr binding sites, and it interacted strongly with Fnr_{D154A}, resulting in a significant band shift. For substrate H-2, removal of the upstream -149.5 Fnr binding site severely reduced its interaction with Fnr_{D154A}. Thus, the binding of Fnr_{D154A} to substrates R-1, R-2 and H-1 was indeed specific.

With binding of Fnr to the *ravA* promoter established, a β -galactosidase transcriptional reporter based colorimetric assay was used to evaluate each of the two identified Fnr-binding sites in regulating the expression of *RavA* and *ViaA*. The *lacZ* gene that encodes β -galactosidase was placed downstream of the native *ravA* (i.e. *ravAviaA*) promoter to create pP_{*ravA*}-*lacZ*. Two additional plasmids were also used for determining the influence of each of the two Fnr-binding sites: pP_{*ravAm1*}-*lacZ*, which has the -72.5 Fnr site replaced with a 14-bp non-native sequence comprised of a *NheI* restriction site flanked by random bases on both ends; and pP_{*ravAm2*}-*lacZ*,

which has the -188.5 Fnr site mutated, while its -72.5 site retains its native sequence (Fig. 2H; see Methods for details). *E. coli* EDCM 367 cells (MG1655 *lacZ*, *lacY*) transformed with these constructs were grown under oxygen-limiting condition, and the cell lysates generated from them subjected to the Miller assay to measure the β -galactosidase activity. A *lacZ* construct lacking the *ravA* promoter (p Δ P-*lacZ*) was used to observe background color development unrelated to β -galactosidase production. An EDCM 367 Δ *fnr* strain transformed with pP_{*ravA*}-*lacZ* was used as a control for Fnr-independent *lacZ* transcription due to the activity of other unidentified transcriptional regulators on the native *ravA* promoter. As shown in Figure 2I, the presence of Fnr in the cell contributes to about 50% increase in β -galactosidase activity, and correspondingly in *lacZ* expression, while under the control of the native *ravA* promoter. This difference accounts for the expression of *lacZ* that is Fnr-dependent, and agrees with our RavA-ViaA expression profile during oxygen-limiting growth as discussed above (Fig. 1B). Importantly, abolishment of the -72.5 Fnr recognition sequence in pP_{*ravAm1*}-*lacZ* led to a complete loss of the Fnr-dependent *lacZ* expression despite the presence of Fnr, and resulted in a β -galactosidase activity which resembles that obtained from the EDCM 367 Δ *fnr* + pP_{*ravA*}-*lacZ* control. In contrast, abolishment of the -188.5 site resulted in only a mild reduction in Fnr-dependent *lacZ* expression, which remained ~24% higher than that of EDCM 367 Δ *fnr* + pP_{*ravA*}-*lacZ*. Thus, the -72.5 Fnr site is revealed to be the primary site for the Fnr-dependent induction of the *ravA* promoter, while the -188.5 site plays a secondary role. This is consistent with our EMSA result, which shows that binding of Fnr_{D154A} to the *ravA* promoter occurs primarily on the -72.5 Fnr site (Fig. 2D).

In the time course analysis for RavA levels (Fig. 1B) some amount of RavA was observed to be present in the absence of Fnr. Similarly, a basal level of β -galactosidase activity was observed in the Fnr knockout strains (Fig. 2I). It is conceivable, not accounting for post-

translational regulation of the protein levels, that other transcription factors may play a part in the expression and regulation of the *ravAviaA* operon. Along with the Fnr-binding sites mentioned above, a seven nucleotide sequence centered 96 nucleotides upstream of the RavA open reading frame was found to match the consensus sequence for the NarL transcription factor (Fig. 2A) [39]. However, the mutation of this proposed recognition sequence had no effect on β -galactosidase activity (not shown).

ViaA physically interacts with uncomplexed FrdA in oxygen-starved cells and the interaction is modulated by RavA

Next, given that RavA and ViaA are induced primarily by Fnr under oxygen-limiting conditions (Fig. 1 and 2), we carried out experiments to identify physical interactors of RavA and ViaA under these conditions, particularly those that are also upregulated by Fnr. To this end, strains that express endogenous C-terminally SPA-tagged proteins were used [40], followed by the detection of RavA and/or ViaA bound to the isolated protein complexes through Western blotting. The SPA-tag is a dual-affinity tag consisting of 3xFLAG and a calmodulin binding peptide motif separated by a cleavage site for tobacco etch virus (TEV) protease. The choices of proteins to be tagged were based on the results of our co-expression profiling for *ravA* and *viaA*, as well as, on the several high-throughput studies that we previously carried out [9, 17].

As shown in Figure 3A, among the 22 proteins that were successfully SPA-tagged, ViaA (untagged; MW = 56 kDa) was observed to interact strongly with SPA-tagged FrdA. FrdA is the flavin adenine dinucleotide (FAD)-binding component of the fumarate reductase complex (FrdABCD) that is involved in anaerobic respiration [18]. No ViaA was observed when FrdA-SPA pull-down was repeated in Δ *viaA* cells (Fig. 3B), which confirms the validity of the

observed ViaA-FrdA interaction. None of the SPA-tagged proteins interacted with RavA, with the only exception being LdcI-SPA (data not shown), which agrees with our previous report [6]. In addition, we had previously shown that RavA only interacts weakly or transiently with ViaA [6], and accordingly, no ViaA was brought down with RavA-SPA, and *vice versa* (data not shown).

In the FrdA-SPA strain, the expression of the Fe-S cluster-containing subunit of fumarate reductase, FrdB, was compromised due to the introduction of the SPA tag (Fig. 3B). Similarly, given that both *frdC* and *frdD* are located downstream of *frdB*, expression of FrdC and FrdD were presumed to be compromised as well; however, antibodies against these two proteins were not available for us to test this. Hence, the interaction between ViaA and FrdA-SPA does not require endogenous FrdBCD as ViaA seems to bind free FrdA.

To further investigate this observation, the FrdA-SPA strain was transformed with plasmids that overexpress either the FrdB alone or the FrdBCD subunits of the Frd complex, and the immunoprecipitation experiments were repeated. No interaction was observed between FrdA and ViaA in the presence of FrdB or FrdBCD (Fig. 3C; IP). We interpret these results to mean that ViaA binds free FrdA and not FrdA in an FrdAB or FrdABCD complex.

In light of the interaction of FrdA-SPA with ViaA, the potential role of RavA in modulating this interaction was also investigated. The immunoprecipitation experiments were repeated for FrdA-SPA strain transformed with the plasmids pRV or pR_{K52Q}V. The pRV plasmid expresses wild type ViaA and RavA. The pR_{K52Q}V plasmid expresses WT ViaA and a mutant RavA in which the lysine residue of the Walker A motif is mutated to glutamine, rendering the protein ATPase inactive. As shown in Fig. 3D, protein levels were the same (input), however, more ViaA and RavA bound FrdA-SPA in the presence of ATPase deficient RavA. We speculate

that RavA ATPase activity disrupts or weakens the ViaA-FrdA interaction.

ViaA associates with RavA through its N-terminal domain and with FrdA through its C-terminal VWA domain

The pulldowns in Figure 3 point towards ViaA as the common partner binding to FrdA and RavA in a potential tertiary complex, as RavA alone is not pulled down by FrdA. To verify direct interactions among FrdA and ViaA and to identify the role of ViaA domains in mediating the transient RavA-ViaA-FrdA complex formation, co-immunoprecipitation experiments were performed with purified proteins. A schematic of the ViaA domain arrangement is shown in Fig. 4A. This was obtained based on sequence alignment of ViaA from several bacterial species and on partial protease digestion (not shown). The VWA domain of ViaA is at the C-terminus [6] (CTV). The N-terminal domain of ViaA (NTV) appears to be novel with little sequence similarity to any characterized protein. The purified isolated NTV domain was stable (see below), but CTV was highly insoluble and was fused to a NusA tag to stabilize it (see Methods).

Pulldown experiments were carried out with the FrdA-SPA construct used as the bait. Figure 4B depicts the results whereby purified RavA, ViaA, and its CTV and NTV domains were used as prey for the pulldowns with either FrdA-SPA bound to anti-FLAG M2-affinity beads or using the beads without any bound protein. After washing, proteins were eluted using TEV protease. The protease cleaves the FLAG-tag moiety of the SPA-tag fused to the C-terminal of FrdA. In the instance where no protein was bound onto the beads, mock elutions were performed under the same conditions. No significant interaction was observed between RavA and FrdA, consistent with the results in Fig. 3A and 3D. On the other hand, ViaA eluted with FrdA, thus showing a direct interaction between the two proteins. More specifically, despite

some basal level of association with the beads, an increase in NusA-CTV co-elution was seen in the presence of FrdA while the NTV did not bind FrdA-SPA at all. Also, NusA alone did not bind FrdA. These pulldowns show that ViaA associates with FrdA through its VWA domain.

Based on the above results, since CTV in ViaA binds FrdA, we speculated that NTV in ViaA binds RavA. We initially biochemically characterized the NTV domain. Like ViaA, NTV (theoretical MW of 36 kDa) was found as a mainly monomeric protein by size exclusion chromatography (Fig. 5A) and sedimentation equilibrium analytical ultracentrifugation (Fig. 5B). NTV was found to be enriched in α -helices (32%) and β -sheets (22%) at 20°C as measured by circular dichroism spectroscopy (Fig. 5C) and to be highly stable with a T_m of 66.1°C under the conditions tested (Fig. 5D). Next, we made use of our previous observation that RavA ATPase activity is enhanced by ViaA [6] to check for the potential interaction of NTV with RavA. RavA ATPase activity was tested in the presence of ViaA and its different domain constructs. The activity of RavA (measured at 0.5 μ M protomer concentration) was increased to similar levels by equimolar concentration of full length ViaA protein or NTV (Fig. 5E). The presence of NusA-CTV or NusA had no significant effect on RavA ATPase (Fig. 5E). Hence, the results indicate that ViaA associates with RavA through its NTV segment. Further, by measuring the ATPase activity enhancement of RavA at different concentrations of the full length ViaA protein or the NTV domain (Fig. 5F), we obtained apparent dissociation constants of 0.15 μ M and 0.55 μ M for the ViaA-RavA and NTV-RavA associations, respectively.

Taken together, the results of Figures 4 and 5 show that ViaA can be considered as an adaptor protein that interacts with RavA via its NTV and with FrdA via its CTV.

RavA-ViaA regulate the activity of the Frd complex in *E. coli*

Both the physical interaction between ViaA and FrdA-SPA, and the antagonistic effect of RavA on the FrdA-ViaA interaction suggest that RavA-ViaA might functionally modulate the activity of the Frd complex. To test this possibility, inverted membrane vesicles were isolated from anaerobically grown MG1655 cells expressing different levels of RavA and/or ViaA. The isolated vesicles containing the Frd complex were then examined for differences in fumarate reductase activity *in vitro* by measuring the oxidation of benzyl viologen (BV) in the presence of fumarate (see Methods).

As shown in Figure 6A, vesicles isolated from $\Delta ravA viaA$ and $\Delta ravA viaA + p11$ (p11 is an empty vector) strains showed an increase greater than 43% in Frd activity compared to WT vesicles. In contrast, addition of RavA and ViaA ($\Delta ravA viaA + pRV$) resulted in reduction of Frd activity to near WT levels. As a control, assay performed in the absence of fumarate or with vesicles from $\Delta frdA::kan^R$ strain did not show any fumarate reductase activity, which highlights the specificity of this assay in capturing only the activity of the Frd complex. Importantly, neither RavA nor ViaA had any observable effects on the expression levels of FrdA (and presumably FrdB, FrdC, and FrdD) (Fig. 6B). Hence, RavA and ViaA play a role in mediating the rate of fumarate reduction by the Frd complex by possibly regulating its maturation and assembly.

Discussion

In this study, we elucidated a novel functional association of the MoxR protein RavA and its VWA partner, ViaA, from *E. coli* with the fumarate reductase complex during anaerobiosis. The interaction between the RavA-ViaA system and the Frd complex modulates the activity of the complex (Fig. 6). This association was revealed due to our observation that RavA and ViaA are

overexpressed under oxygen-limiting conditions. Though other transcription factors may also be responsible, the expression of RavA-ViaA during oxygen starvation was found to be primarily inducible by the transcriptional regulator Fnr, which also regulates the expression of the Frd complex as well as other proteins involved in anaerobiosis [29, 41]. Our finding of the regulation of the *ravAviaA* promoter by Fnr is consistent with a recent high throughput study based on a ChIP-chip approach [42].

Importantly, the role of σ^S in the induction of RavA-ViaA expression is significantly diminished and is largely relinquished to Fnr during oxygen-limiting growth. This coincides with a previous report in which the expression of σ^S in *E. coli* MC4100 and MG1655 was shown to decrease during anaerobiosis [43]. Nevertheless, our data indicates that σ^S does have a role in modulating the expression of RavA and ViaA under oxygen limiting conditions. Under these conditions, RavA expression is induced in log phase but then drastically further increases in stationary phase. However, ViaA expression peaks at log phase and then decreases in stationary phase (Fig. 1B). In the absence of σ^S , this biphasic opposing regulation of RavA and ViaA is not observed to a significant extent (Fig. 1B). Hence, σ^S differentially modulates the expression of ViaA and RavA under oxygen starvation. Under these conditions, σ^S might, for example, induce a protease that degrades ViaA but not RavA. Alternatively, given that *ravA-viaA* form an operon, σ^S might indirectly regulate the translation of the *ravA-viaA* mRNA.

In a previous report, we had shown that RavA and ViaA interact both physically and functionally with specific subunits of the NADH:ubiquinone oxidoreductase I (Nuo complex) [9]. RavA-ViaA interact primarily with the FMN (flavin mononucleotide)-binding NuoF subunit under aerobic conditions, and with the fused NuoCD subunit under anaerobic conditions [9]. Importantly, the Nuo complex is known to be involved in both the aerobic and the anaerobic

respiration of *E. coli* [14, 15]. It has also been shown that the coupling between the Nuo complex and the Frd complex is important for the electron transfer from NADH to fumarate during anaerobic respiration of *E. coli* [16]. Taken together, our results support a potential regulatory role of RavA-ViaA in the anaerobic utilization of fumarate via its interaction with both the Nuo and Frd complexes.

Our current working model of the effect of RavA-ViaA on the assembly of the Frd complex is depicted in Figure 7. We had shown previously that ViaA tends to associate with the bacterial inner membranes [9]. Hence, we speculate that an initial interaction occurs between the flavoenzymatic FrdA subunit of the Frd complex and ViaA at the inner membranes. This occurs with free FrdA in the absence of FrdB, as the presence of FrdB precludes this association. Though RavA was not observed to directly bind FrdA, a tertiary complex of RavA-ViaA-FrdA was clearly seen when the ATPase deficient mutant of RavA was used (Fig. 3D). ViaA acts as an adaptor in this complex by using its N-terminal domain to bind to RavA and its C-terminal VWA domain to bind FrdA (Fig. 4 and 5). The ATPase activity of RavA seems to facilitate the disassembly of the ViaA-FrdA association (Fig. 3D). If FrdB is then available, the free FrdA can associate with FrdB, after which the FrdAB subcomplex interacts with FrdCD to form the complete Frd complex [18]. The association of RavA-ViaA with FrdA leads to the regulation of the Frd activity as seen in Figure 6A. We propose that ViaA captures free FrdA to maintain its stability or to allow for the proper covalent attachment of cofactors to FrdA or FrdB proteins before their assembly into the full Frd complex. The association of ViaA with FrdA might also be required to delay the assembly of the FrdAB subcomplex and provide time for the FrdCD subcomplex to form and insert into the inner cell membrane [18].

Such an interactive system of an ATPase and VWA partner has recently been observed in

the chemolithoautotroph *Acidithiobacillus ferrooxidans* [44]. The CO₂ assimilating RuBisCo enzyme of *A. ferrooxidans* is activated by the MoxR AAA+ CbbQ protein. Importantly, the VWA domain-containing CbbO protein is required to bind to RuBisCo via the VWA domain to recruit CbbQ to its substrate [44].

Considering that MoxR proteins generally act as chaperones for specific targets [1, 2], it is tempting to speculate that RavA-ViaA fulfill this function by regulating the maturation process of specific Frd and Nuo subunits or the assembly of these subunits into respiratory subcomplexes or the assembly of Frd and Nuo complexes into a supercomplex. In this regard, it is interesting to note that the Frd complex works in conjunction with the Nuo complex in the electron transfer from NADH to fumarate during the anaerobic respiration of fumarate [16, 18]. In conclusion, the proposed cellular activity of RavA-ViaA adds to a developing pattern of how MoxR AAA+ ATPases might function in nature.

Materials and Methods

Bacterial strains and plasmids

All bacterial strains and plasmids used are listed in Table 2. Primers used in the construction of these strains and plasmids are also listed in Table 2. All knockout (KO) mutants of the *ravA/viaA* open reading frames were constructed as previously described [6] by employing lambda red recombination [45] and P1 phage transduction [46]. EDCM 367 cells were generously provided by Dr. Christophe Merlin (University of Lorraine) [47]. MG1655 $\Delta frdA::kan^R$, MG1655 $\Delta rpoS::kan^R$ and EDCM $\Delta frdA::kan^R$ were constructed via P1 phage transduction. The required *frdA* and *rpoS* KO cassettes that carry the *kan^R* gene were obtained from BW25113 $\Delta frdA::kan^R$ and $\Delta rpoS::kan^R$, respectively, both of which came from the KEIO collection [48, 49]. All

DY330 strains expressing C-terminal SPA-tagged proteins were a generous gift from Dr. Andrew Emili (University of Toronto) and were constructed using the protocols described in Zeghouf *et al.* [50]. DY330 FrdA-SPA Δ *viaA::cat* was constructed by P1 phage transduction. The required *viaA* KO cassette was obtained from MG1655 Δ *viaA::cat* that was used in a previous study [6].

The plasmid pRV (p11-*ravAp-ravAviaA*) was constructed as described in our previous work [6]. The plasmid pR_{K52Q}V was generated by QuikChange site-directed mutagenesis (Stratagene) using the primers RavA K52Q F and RavA K52Q R (Table 2). Similarly, for the plasmids pfrdB (p11-*frdp-frdB*) and pfrdBCD (p11-*frdp-frdBCD*), all inserts were PCR-amplified using the common forward primer FrdB NheI F (Table 2). The reverse primers FrdB XbaI R and FrdD XbaI R (Table 2) were used for pfrdB and pfrdBCD, respectively. The inserts were then cloned into p11-*frdp* using the restriction enzymes NheI and XbaI (New England Biolabs). All constructs were verified by DNA sequencing.

For high, inducible expression of desired proteins, T7 promoter controlled constructs (Table 2) were created using common amplification and cloning techniques. Proteins for overexpression include the FrdA-SPA fusion in the pET3aTr vector, NusA-ViaA fusion in the pETm-60 vector, N-terminal of ViaA (NTV, residues 1-311) in p11, fusion of C-terminal of ViaA (residues 312-483) with NusA (NusA-CTV) in pETm-60 and the RavA protein in p11.

The plasmid pP_{*ravA*}-*lacZ* (Table 2) was constructed with the cloning vector pETm-60 [51]. Expression of *lacZ* is placed under the control of the *ravA* promoter immediately upstream. To construct the plasmid, a fragment that contains the T7 promoter, *lacI*, and 5' half of the *nusA* gene in the original pETm-60 was first removed using StuI and BglII, and the modified vector religated by blunt-end ligation. Next, a 363-bp fragment immediately upstream of the *ravA* ORF,

which covers the *ravA* native promoter, was PCR-amplified using the primers *ravAp* NcoI F and *ravAp* BamHI R (Table 2). The *ravA* promoter was cloned into the modified pETm-60 with NcoI and BamHI. Finally, *lacZ* was PCR-amplified from genomic DNA of *E. coli* using the primers LacZ BamHI F and LacZ NotI R (Table 2). The amplified *lacZ* gene was then cloned directly downstream of the *ravA* promoter with BamHI and NotI to give pP_{*ravA*}-*lacZ*. To generate mutations in the *ravA* promoter in pP_{*ravA*}-*lacZ*, the primers *ravAp*(*fmr1*) F and *ravAp*(*fmr1*) R (Table 2) were used to replace the consensus *fmr* sequence (5'-TTGCTTATTATCAG-3') centered at -72.5, in respect to the transcription start site, with 5'-AGAAGCTAGCAACA-3'. Both primers contained the recognition sequence for NheI (5'-GCTAGC-3'), which allowed for digestion and ligation of the PCR product to form circular plasmids. A similar strategy was used to replace putative Fnr recognition site centered at -188.5 (5'-TTAACCTGGCTCAA-3') with 5'-CAAAGCTAGCAAAC-3', using the primers *ravAp*(*fmr2*) F and *ravAp*(*fmr2*) R. A seven nucleotide site centered at -96 (5'-TACTCCT-3') matching the consensus NarL recognition sequence [39] was replaced with 5'-GCTAGCA-3' using the primer pair *ravAp*(NarLm) F and *ravAp*(NarLm) R.

Protein production and purification

The *E. coli* BL21 Gold (DE3) pLysS (Stratagene) strain was used for high-level expression of desired protein constructs. The NusA-ViaA, NTV, NusA-CTV, RavA and FrdA-SPA proteins were induced by addition of 1 mM IPTG to cell cultures grown to mid-log phase at 37°C. The cultures were grown overnight (~16 hrs) at 18°C. After induction, cells were harvested by centrifugation and stored at -80°C.

Nickel affinity chromatography was performed to purify NusA-ViaA, NTV, NusA-CTV,

and RavA constructs each of which contained a cleavable polyhistidine (6xHis) tag. As the CTV separated from the NusA protein was not soluble, the NusA-CTV fusion protein was stored at -80°C for further use without removing the NusA-tag. Tobacco etch virus (TEV) protease was used in a 1:20 molar ratio to cleave the 6xHis-tags from NTV and RavA proteins, and to remove the NusA (containing the 6xHis tag) moiety of the NusA-ViaA fusion. Additionally, ion exchange chromatography with Mono S 5/50 HR or Mono Q 5/50 HR columns was performed to further purify RavA and NTV samples, respectively. ViaA protein was separated from NusA using the HiTrap Heparin HP column.

Size exclusion chromatography

For size exclusion chromatography, the Superose 6, 10/300 GL column (GE Healthcare) was used for RavA, ViaA and FrdA proteins. The Superdex 200 10/300 column (GE Healthcare) was used for the NTV and NusA-CTV constructs. Proteins were run in the SEC buffer: 25 mM HEPES (pH 7.5), 300 mM NaCl, 1 mM MgCl₂, 1 mM DTT, 5% (v/v) glycerol. Elution fractions were collected and visualized using SDS-PAGE.

Co-expression profiling of *ravA* and *viaA* in *E. coli*

The expression levels of *ravA* and *viaA* were compared across different experimental conditions to identify genes with similar expression profiles. To this end, a large compendium composed of 445 microarray datasets was obtained from the M3D public database (Build 4 of *E. coli* expression data) [52]. These data were available in the form of Robust Multi Array (RMA) normalized profiles [53], which enables the direct comparison of the expression profiles of different protein-encoding genes across multiple experimental conditions. The Pearson

correlations, used for comparing the similarity of expression profiles, were computed for all 4,125 genes present on the Affymetrix chip against both *ravA* and *viaA*. This allowed the identification of genes that exhibit the most similar expression profiles to the seed set of genes. Due to the large number of conditions in the compendium, a conservative cut-off of 0.5 was adopted as the correlation threshold to identify the functional links to the seed genes. All functional annotations were obtained from publicly available online databases, such as EcoCyc [54], UniProtKB [55] and RegulonDB [56].

Expression analysis of RavA and ViaA in *E. coli* under aerobic and oxygen-limiting conditions

E. coli MG1655 WT, $\Delta fnr::kan^R$, $\Delta rpoS::kan^R$ and $\Delta ravAviaA$ were grown in Luria-Bertani (LB) media (10 g/L bacto-tryptone, 5 g/L yeast extract, and 10 g/L sodium chloride) at 37 °C either aerobically in 200-mL culture flasks with vigorous shaking, or under oxygen-limiting condition in 60-mL disposable syringes sealed with sterile end caps with gentle agitation. All cultures were inoculated with single colonies grown overnight on LB-agar plates. Growth of cells was tracked by monitoring the changes in OD₆₀₀ at specific time points. For each time point, an aliquot of the cells was harvested by centrifugation and flash-frozen in liquid nitrogen until use. To determine the levels of RavA and ViaA proteins in cells, the cell pellets collected were thawed on ice and then resuspended in 0.1 M potassium phosphate (pH 7.5) supplemented with 0.1 M sodium chloride. The volume of each sample was adjusted to give a final cell count of approximately 3.8×10^9 cells/mL as determined by OD₆₀₀. Cells were lysed by sonication, followed by treatment with 4 × SDS-PAGE sample buffer (200 mM TrisHCl, pH 6.8, 8% SDS, 0.4% bromophenol blue, 40% glycerol, and 400 mM β-mercaptoethanol) and separated on 10% or 12%

polyacrylamide gels. The levels of RavA and ViaA were analyzed by Western blotting. A 70-kDa cross-reacting band in the α -ViaA blot was used as the loading control.

Electromobility shift assay (EMSA)

The *E. coli* Fnr mutant, Fnr_{D154A}, was expressed from the plasmid pPK824 (pET11a-*fnr*_{D154A}) in strain PK22 lacking *fnr* (Table 2) and purified as described in [34], except that SP sepharose (GE Health Sciences) was used in place of BioRex-70 during the first round of purification. Fnr_{D154A} was used in this assay because it retains the same specificity and affinity as WT Fnr for binding to the Fnr consensus DNA sequence even under aerobic conditions [34]. All DNA substrates required were PCR-amplified using the appropriate primers listed in Table 2.

To detect the binding of Fnr_{D154A} to the DNA substrates, 3 nM of DNA substrate was incubated with 60 nM Fnr_{D154A} in 20 mM Tris-acetate (pH 7.5) supplemented with 40 mM KCl, 1 mM MgCl₂ and 5% (v:v) glycerol for 30 minutes at 37 °C. All samples were electrophoresed at 4 °C in a 4% polyacrylamide native gel supplemented with 10% polyethylene glycol with 20 mM Tris-acetate (pH 8.0) as the running buffer. The gel was then incubated in 20 mM Tris-acetate (pH 8.0) supplemented with the RedSafe DNA stain (Chembio) with gentle agitation at room temperature to stain the DNA bands contained within. Visualization of the DNA bands was done using the GelDoc 2000 (BioRad).

β -Galactosidase reporter assay

To quantify the effect of Fnr on the recognized regulatory sequences in the RavA-ViaA promoter region, *lacZ* expression under the control of the native and mutated *ravA* promoter was monitored using previously established protocols [57]. The pP_{*ravA*}-*lacZ* plasmid (Table 2) that

expresses *lacZ* under the control of the native *ravA* promoter, a no-promoter control (p Δ P-*lacZ*), promoter with mutated Fnr recognition sites (pP_{*ravAm1*}-*lacZ* and pP_{*ravAm2*}-*lacZ*) or a mutated NarL consensus matching sequence (pP_{*ravAm3*}-*lacZ*) were constructed as described above. These plasmids were introduced into the EDCM 367 (*E. coli* MG1655 *lacZ*, *lacY*) and pP_{*ravA*}-*lacZ* was also transformed into EDCM 367 Δ *fnr*.

Cells were inoculated from overnight starter cultures and then grown under oxygen-limiting condition in LB supplemented with 1% (v/v) glycerol and 50 mM sodium fumarate in sealed, sterile tubes. The cultures were grown until their OD₆₀₀ reached ~0.5. At which point, three 1-mL samples were collected for each culture. The cells were pelleted and lysed using the permeabilization solution (0.8 mg/mL cetyl trimethyl ammonium bromide (CTAB), 0.4 mg/mL sodium deoxycholate, 100 mM Na₂HPO₄, 20 mM KCl, 2 mM MgSO₄, and 5.4 μ L/mL β -mercaptoethanol). The substrate solution (1 mg/mL ortho-nitrophenyl- β -galactoside (ONPG), 60 mM Na₂HPO₄, 40 mM NaH₂PO₄, 20 μ g/ μ L CTAB, 10 μ g /mL sodium deoxycholate 2.7 μ L/mL β -mercaptoethanol) was added to the lysed samples and the reaction was run for no more than 120 minutes. 700 μ L of 1 M sodium carbonate was added to stop the reaction after sufficient color had developed. The samples were centrifuged to remove cell debris and 200 μ L of supernatant was then transferred to a 96-well plate and the absorbance at 420 nm was measured. Miller units were calculated using the following formula [46]:

$$\text{Miller units} = 1000 \times [(\text{Abs}_{450}) / (\text{OD}_{600} \times \text{cell culture volume used in mL} \times \text{reaction time in minutes})]$$

Immunoprecipitation by SPA-tagged bait proteins

Endogenous Sequential Peptide Affinity (SPA)-tagging of proteins was carried out in *E. coli* DY330 using the protocols described in Zeghouf *et al.* [50]. Cells with confirmed incorporation

of the SPA-tags at the C-terminus of targeted proteins were grown in LB media at 30 °C in sealed sterile 50-mL centrifuge tubes for over 24 hours. Cells were then harvested by centrifugation at 4°C and resuspended in buffer A (25 mM TrisHCl, pH 7.5, 100 mM KCl, 10 mM MgCl₂, 1 mM CaCl₂, 0.2 mM EDTA, 1% Triton X-100, 10% glycerol, and 0.5 mM DTT) supplemented with 1 mg/mL lysozyme (BioShop) and 0.1 U/mL DNaseI (Fermentas). After incubation on ice for 15 minutes, cells were lysed by sonication. Total soluble proteins were isolated from the crude cell lysate by centrifugation. The SPA-tagged proteins and the stably associated proteins were purified using ANTI-FLAG M2 Affinity Beads (Sigma-Aldrich) following the manufacturer's protocols, which were then analyzed by SDS-PAGE and Western blotting.

C-terminally SPA-tagged FrdA was also used as bait to verify interactions with purified proteins. An FrdA-SPA fusion construct, under the control of a T7 promoter in the pET3aTr plasmid, was induced using IPTG in BL21 Gold (DE3) pLysS cells. The expression was carried out for 16 hrs at 18°C. Cells were harvested and resuspended in the lysis buffer mentioned above and lysed by sonication. After removal of cell debris, the supernatant collected from 1 mL of culture was incubated with 40 µL of ANTI-FLAG M2 affinity beads overnight at 4°C. The beads were placed in Bio-Spin® chromatography columns and unbound protein was washed away with 5 mL of buffer A. Next, 200 µL of buffer containing one of the following: 1 µM RavA, 1 µM ViaA, 1 µM NTV, 0.1 µM NusA-CTV or 0.1 µM NusA was added to the beads and incubated with gentle shaking for 4 hrs. The beads were again washed to remove unbound protein. Elution was performed overnight to release FrdA-SPA from the beads by incubation of beads in buffer A containing 200 µL of 0.1 mg/mL TEV protease.

Circular dichroism spectroscopy

The NTV protein was prepared at 0.4 mg/mL in CD buffer (25 mM HEPES pH 7.5, and 50 mM NaF). 200 μ L of sample was used with a 1 mm pathlength quartz cuvette. The Jasco J-810 spectropolarimeter was used for measurement. For the thermal melt profile, the ellipticity was measured at 222 nm from 20°C to 80°C as temperature was increased by 1°C/minute. Wavelengths scans were performed at 5°C intervals from 250 nm to 200 nm at a 1 nm pitch and a speed of 50 nm/min. Wavelength scans were performed in triplicate and averaged. The curves were twice smoothed using the Savitzky-Golay algorithm with a convolution width of 25 [58]. To estimate the secondary structure composition, the BeStSel single spectrum analysis and fold recognition tool was utilized [59].

Western Blotting

Samples to be analyzed were first separated using a 10% or 12% SDS-PAGE gels. The protein bands were then transferred onto an Amersham Hybond-P PVDF membrane (GE Healthcare) using the TE77X Semi-dry Transfer Unit (Hoefer Inc.) following manufacturer's instructions. The membrane was then blocked, washed and incubated with the appropriate antibodies as required, using standard protocols. The polyclonal rabbit antibodies against RavA and ViaA were generated at the Division of Comparative Medicine, University of Toronto. The polyclonal rabbit antibodies against FrdA and FrdB in *E. coli* were generously provided by Professor Joel Weiner (University of Alberta, Edmonton, Canada). The monoclonal mouse antibody against the FLAG tag was purchased from Sigma-Aldrich. Commercially available monoclonal antibody against the calmodulin binding peptide (CBP) (EMD Millipore) was used to detect the FrdA-SPA construct and a NusA monoclonal antibody (EMD Millipore) was used to detect either

NusA protein or the NusA-CTV fusion.

Analytical Ultracentrifugation

A sedimentation equilibrium run was performed on Beckman Optima XL-A analytical ultracentrifuge. The NTV construct was run at concentrations of 1.0 mg/mL, 0.5 mg/mL and 0.25 mg/mL in a buffer containing 25 mM HEPES, 300 mM NaCl and 1 mM DTT. The experiment was run at 4°C for 27 hours each at 14000 and 16000 rpm using An-60 Ti rotor. Protein concentrations across the length of the cell were measured using absorbance at 280 nm. Origin 4.1 software was used to analyze the data. The partial specific volume, solvent density and viscosity were calculated using SEDNTERP [60].

RavA ATPase assay

The ATPase activity of RavA, in the presence or absence of ViaA and its domains, was tested using the ATP/NADH coupled assay [61]. The ATPase buffer with the following final components was used: 0.2 mM NADH, 3 mM phosphoenolpyruvate, 4.7 U/mL pyruvate kinase, 7.4 U/mL lactate dehydrogenase, 5 mM MgCl₂, 25 mM HEPES, 50 mM NaCl. The relevant proteins were placed in ATPase buffer with 5 mM ATP. Unless indicated, 0.5 μM of proteins were used. The 150 μL reactions were carried out at 37°C in a clear 96-well plate on the SpectraMax 340PC384 microplate reader, absorbance was measured at 340 nm for 20 minutes at 20-second intervals.

Fumarate reductase activity assay

E. coli MG1655 WT, Δ ravAviaA, Δ ravAviaA + p11, , Δ ravAviaA + pRV, Δ ravAviaA + pR_{K52Q}V

and BW25113 Δ *frdA::kan^R* were grown under oxygen-limiting condition inside sealed, sterilized containers in EZ-defined rich media [62] supplemented with 1% (v:v) glycerol and 50 mM sodium fumarate at 37 °C over 16 hours. Cells were then harvested by centrifugation, re-suspended in 0.1 M sodium phosphate buffer (pH 7) and lysed by two passages through a French Press (Thermo Spectronic) at 18000 lb/in². Cell lysis by French Press generates inside-out membrane vesicles. Cell debris was removed by centrifugation. To isolate the membrane vesicles, the cleared cell lysate was subjected to ultracentrifugation at 150,000 × g at 4 °C for 1.5 hours. The pelleted membrane vesicles were resuspended in 0.1 M sodium phosphate buffer (pH 7), flash-frozen with liquid nitrogen, and stored at -80 °C until use.

To measure the activity of endogenously expressed fumarate reductase in the isolated inside-out membrane vesicles, a modified version of the benzyl viologen (BV) colorimetric assay described in [63] was used. Briefly, 0.125 mM (final concentration) BV was first reduced with 1.5 mM (final concentration) Na₂S₂O₄ in 0.1 M sodium phosphate (pH 7), followed by the addition of 60 µg/mL of membrane vesicles. To initiate the reaction, 20 mM (final concentration) sodium fumarate was added and the mixture was homogenized by gentle pipetting to minimize oxidation of BV by air. Fumarate reductase activity was tracked by monitoring the loss of the purple color as BV was oxidized in the presence of fumarate. This was done by measuring absorbance at 500 nm of the reaction mixture in a standard 1-cm cuvette using the CARY300 UV-Vis Spectrophotometer (Agilent Technologies). Measurements were taken every second for 3 minutes at room temperature. Fumarate reductase activity was calculated using the equation 1 U = 1 µmol BV oxidized/min, with the extinction coefficient of BV = 7.8 × 10³ M⁻¹·cm⁻¹ [63]. The results were then normalized to the amount of membrane vesicles used to allow comparison between samples.

ACCEPTED MANUSCRIPT

ACKNOWLEDGEMENTS

KSW is the recipient of a fellowship from the Canadian Institutes of Health Research (CIHR) Strategic Training Program in Protein Folding and Interaction Dynamics: Principles and Diseases (TGF-53910) and a Doctoral Completion Award from the University of Toronto. Vaibhav Bhandari is the recipient of the Natural Science and Engineering Science Council of Canada's (NSERC) Postgraduate Scholarship-Doctoral (PGS-D) award and was the recipient of a Jaro Sodek Award – Ontario Student Opportunity Trust Fund (OSOTF) fellowship from the Department of Biochemistry at the University of Toronto. This work was supported by a grant from the Canadian Institutes of Health Research (MOP-130374) to WAH.

Figure legends

Figure 1. Co-expression profiles and expression analysis for RavA and ViaA

(A) Shown are genes that have similar expression profiles as *ravA* and *viaA*. Single or multiple genes enclosed in rectangular boxes denote the constituents of monocistronic (only one gene included in its own box) or polycistronic operons (multiple genes in one box), respectively. Genes from the same polycistronic operon that are classified to a different co-expression category are linked with broken lines. All genes that are under the control of the transcriptional regulator Fnr are denoted with an asterisk (*).

(B) Western blots of RavA and ViaA for aerobically grown cells (shown on the left) and cells grown under oxygen limitation (shown on the right). All strains were grown in LB media. The time points at which cells were harvested are as indicated at the top. The $\Delta ravA viaA$ cells harvested after 24 hours of growth were used to provide a reference for expressed RavA and ViaA. A cross-reacting band in the α -ViaA blots (at 70-kDa) that remains consistent at all the time points was used as the loading control.

Figure 2. The *ravA viaA* promoter region and its regulation by Fnr

(A) Sequence for the *ravA* and nearby *kup* (encodes the K⁺ transporter; shown here in reverse complement) open reading frames are colored in purple and green, respectively. The σ^S consensus sequence in red [64], transcription start site in blue [65] and the Shine-Dalgarno sequence in black box are indicated as shown. The potential Fnr binding sites are underlined with pink and a putative seven-nucleotide stretch of sequence matching the NarL consensus site is underlined in green. The genomic coordinates are given to the left of each line.

(B) Genetic layout for the *ravA-viaA* and *kup* genes is represented, highlighting the position of the σ^S consensus sequence, the two putative Fnr binding sites (pink bars) and a site matching the NarL consensus sequence (green bar).

(C, E, F) Schematic representations of the DNA substrates R-1, R-2 and R-3 for the *ravAviaA* promoter region (C), F-1 for the *fepD* promoter region (E), and H-1, H-2 and H-3 for the *hypBCDE* promoter region (F). Both putative and confirmed binding sites for Fnr are indicated with black boxes as illustrated and their DNA sequences are shown below. Bases that are underlined represent the half-sites (both putative and confirmed) that are crucial for Fnr binding [33, 38]. The genomic region covered by each DNA substrate is indicated at both ends with the corresponding *E. coli* K-12 genome coordinates. Bent arrows represent the transcriptional start sites (+1).

(D, G) EMSA results using substrates R-1, R-2 and R-3 (D), and F-1, H-1, H-2 and H-3 (G). The absence (-) and presence (+) of Fnr_{D154A} in the reaction mixture are as indicated at the top. The origins of all DNA substrates used are as shown. The molecular weights of the DNA markers used are shown on the left of the gel.

(H) The mutations made at the Fnr-binding sites within the *ravA* promoter region are listed.

(I) A graph representing the β -galactosidase activity levels in cells grown under oxygen limitation are shown when under control of the indicated promoter region. Either EDCM 367 (WT) cells or the EDCM 367 Δfnr (Δfnr) strains were used. β -galactosidase, encoded by *lacZ*, expression was under the control of no promoter (p ΔP -*lacZ*), *ravA* native promoter (pP_{*ravA*}-*lacZ*) or the RavA promoters mutated at either of two Fnr-binding sites (pP_{*ravAm1*}-*lacZ*, pP_{*ravAm2*}-*lacZ*). P-values comparing the Δfnr + pP_{*ravA*}-*lacZ*, WT + pP_{*ravAm1*}-*lacZ* and WT + pP_{*ravAm2*}-*lacZ* with WT + pP_{*ravA*}-*lacZ* are indicated with * and noted at the top of the graph.

Figure 3. The interaction of ViaA with FrdA

(A) Initial screen to identify physical interactors of ViaA in DY330 cells grown under oxygen limitation in LB. SPA tag was fused to the endogenous genes. The identities of bait proteins are as given at the top. “*” denotes ViaA-SPA; “†” denotes cross-reacting bands in the α -ViaA blot. The ViaA band is indicated by an arrow.

(B) Confirmation of the interaction between ViaA and FrdA-SPA. Note that FrdB expression was abolished due to the introduction of the SPA tag. All cells were grown under oxygen limitation in LB. Identities of the strains are given at the top. Total refers to soluble proteins from total cell lysate; IP refers to proteins found in the immunoprecipitation of FrdA-SPA.

(C) Western blots of total RavA, ViaA, FrdA-SPA, and FrdB in DY330 FrdA-SPA strain grown under oxygen limitation and after immunoprecipitation of FrdA-SPA. Sol. Ptn. = soluble proteins; IP = immunoprecipitation.

(D) Western blots for total RavA, ViaA and FrdA in DY330 FrdA-SPA strain transformed with pRV or pR_{K52Q}V grown under oxygen limitation and after immunoprecipitation of FrdA-SPA.

Figure 4. Pulldown assays mapping the interaction of ViaA domains with RavA and FrdA

(A) A schematic of the ViaA protein showing the domain boundaries of NTV (residues 1-311) and CTV (312-483).

(B) Western blots are shown for the immunoprecipitation performed with either FrdA-SPA bound onto FLAG-affinity beads or with empty beads. Purified RavA, ViaA, NTV, NusA-CTV or NusA proteins were added to the beads as indicated. The antibody used for detection is noted on the left with the respective detected protein indicated on the right. High and low exposure

blots are shown for clarity.

Figure 5. Characterizing the interaction of NTV with RavA

(A) Size exclusion chromatography (SEC) of the ViaA and FrdA proteins on Superose 6 column, and of NTV on Superdex 200 column. Molecular weight markers are indicated on the top of each panel with the elution volumes noted on the bottom.

(B) The lower panel shows the analytical ultracentrifugation sedimentation equilibrium data for NTV at 14 μM at 4°C. The solid line is the theoretical fit to the data using a single species function. The molecular weight (MW) and the 95% confidence interval values are given. The upper panel displays residual deviations from the theoretical fit.

(C) Shown are the CD wavelength scans for NTV as a function of temperature.

(D) Thermal melt of NTV monitored by CD at 222 nm. The melting temperature (T_m) is given above the curve.

(E) RavA (0.5 μM) ATPase activity rates in the presence of equimolar amounts of ViaA, NTV, NusA-CTV or NusA proteins. A * indicates that the difference from the ATPase activity of RavA alone is significant, p-value < 0.01.

(F) Change in RavA ATPase activity as a function of ViaA (green) or NTV (blue) concentration.

The data were fit to a single binding site model to obtain an apparent K_d .

Figure 6. RavA-ViaA modulate fumarate reductase activity in oxygen-starved *E. coli* MG1655

(A) Benzyl viologen (BV) assay on inverted membrane vesicles isolated from cells expressing different levels of RavA and ViaA. The strains used are identified below the graph. Three

independent experiments were conducted for each strain. 1 U = 1 μ mol BV oxidized per minute.

P-values < 0.01 were obtained when comparing the $\Delta ravA$ viaA, $\Delta ravA$ viaA + p11, and $\Delta ravA$ viaA + pRV Frd activities with WT activity. This is indicated with *.

(B) Western blotting confirms that protein levels of FrdA remain unchanged upon changes in RavA and ViaA levels.

Figure 7. Model of the function of RavA-ViaA in the modulation of the fumarate reductase respiratory complex assembly

The Frd complex formation is shown along with the proposed contribution of the ViaA and RavA proteins in regulation of complex assembly. As the Frd operon is translated, the FrdC and FrdD proteins are targeted to the inner membrane while FrdA and FrdB are processed in the cytoplasm before they associate with the membrane-bound subunits. Free ViaA mainly associates with the bacterial inner membrane where ViaA interacts with FrdA (1). In the presence of FrdB, ViaA is not observed to associate with FrdA. The ViaA-FrdA interaction is modulated by RavA in an ATP-dependent manner (2). FrdB associates with FrdA (3) and this is followed by FrdAB interacting with FrdCD at the membrane (4) to form a functional respiratory fumarate reductase complex (5).

References

- [1] Snider J, Houry WA. MoxR AAA+ ATPases: a novel family of molecular chaperones? *J Struct Biol.* 2006;156:200-9.
- [2] Wong KS, Houry WA. Novel structural and functional insights into the MoxR family of AAA+ ATPases. *J Struct Biol.* 2012;179:211-21.
- [3] Sutter M, Roberts EW, Gonzalez RC, Bates C, Dawoud S, Landry K, et al. Structural Characterization of a Newly Identified Component of alpha-Carboxysomes: The AAA+ Domain Protein CsoCbbQ. *Sci Rep.* 2015;5:16243.
- [4] Bhuwan M, Arora N, Sharma A, Khubaib M, Pandey S, Chaudhuri TK, et al. Interaction of Mycobacterium tuberculosis Virulence Factor RipA with Chaperone MoxR1 Is Required for Transport through the TAT Secretion System. *MBio.* 2016;7:e02259.
- [5] Whittaker CA, Hynes RO. Distribution and evolution of von Willebrand/integrin A domains: widely dispersed domains with roles in cell adhesion and elsewhere. *Mol Biol Cell.* 2002;13:3369-87.
- [6] Snider J, Gutsche I, Lin M, Baby S, Cox B, Butland G, et al. Formation of a distinctive complex between the inducible bacterial lysine decarboxylase and a novel AAA+ ATPase. *J Biol Chem.* 2006;281:1532-46.
- [7] El Bakkouri M, Gutsche I, Kanjee U, Zhao B, Yu M, Goret G, et al. Structure of RavA MoxR AAA+ protein reveals the design principles of a molecular cage modulating the inducible lysine decarboxylase activity. *Proc Natl Acad Sci U S A.* 2010;107:22499-504.
- [8] Hanson PI, Whiteheart SW. AAA+ proteins: have engine, will work. *Nat Rev Mol Cell Bio.* 2005;6:519-29.
- [9] Wong KS, Snider JD, Graham C, Greenblatt JF, Emili A, Babu M, et al. The MoxR ATPase RavA and its cofactor ViaA interact with the NADH:ubiquinone oxidoreductase I in *Escherichia coli*. *PloS one.* 2014;9:e85529.
- [10] Kanjee U, Gutsche I, Alexopoulos E, Zhao B, El Bakkouri M, Thibault G, et al. Linkage between the bacterial acid stress and stringent responses: the structure of the inducible lysine decarboxylase. *EMBO J.* 2011;30:931-44.
- [11] Malet H, Liu K, El Bakkouri M, Chan SW, Effantin G, Bacia M, et al. Assembly principles of a unique cage formed by hexameric and decameric *E. coli* proteins. *eLife.* 2014;3:e03653.
- [12] Park YK, Bearson B, Bang SH, Bang IS, Foster JW. Internal pH crisis, lysine decarboxylase and the acid tolerance response of *Salmonella typhimurium*. *Mol Microbiol.* 1996;20:605-11.
- [13] Girgis HS, Hottes AK, Tavazoie S. Genetic architecture of intrinsic antibiotic susceptibility. *PloS one.* 2009;4:e5629.

- [14] Unden G, Bongaerts J. Alternative respiratory pathways of *Escherichia coli*: energetics and transcriptional regulation in response to electron acceptors. *Biochim Biophys Acta*. 1997;1320:217-34.
- [15] Price CE, Driessen AJ. Biogenesis of membrane bound respiratory complexes in *Escherichia coli*. *Biochim Biophys Acta*. 2010;1803:748-66.
- [16] Tran QH, Bongaerts J, Vlad D, Unden G. Requirement for the proton-pumping NADH dehydrogenase I of *Escherichia coli* in respiration of NADH to fumarate and its bioenergetic implications. *Eur J Biochem*. 1997;244:155-60.
- [17] Babu M, Arnold R, Bundalovic-Torma C, Gagarinova A, Wong KS, Kumar A, et al. Quantitative genome-wide genetic interaction screens reveal global epistatic relationships of protein complexes in *Escherichia coli*. *PLoS genetics*. 2014;10:e1004120.
- [18] Cecchini G, Schroder I, Gunsalus RP, Maklashina E. Succinate dehydrogenase and fumarate reductase from *Escherichia coli*. *Biochim Biophys Acta*. 2002;1553:140-57.
- [19] Iverson TM, Luna-Chavez C, Croal LR, Cecchini G, Rees DC. Crystallographic studies of the *Escherichia coli* quinol-fumarate reductase with inhibitors bound to the quinol-binding site. *J Biol Chem*. 2002;277:16124-30.
- [20] Iverson TM, Luna-Chavez C, Cecchini G, Rees DC. Structure of the *Escherichia coli* fumarate reductase respiratory complex. *Science*. 1999;284:1961-6.
- [21] Westenberg DJ, Gunsalus RP, Ackrell BA, Cecchini G. Electron transfer from menaquinol to fumarate. Fumarate reductase anchor polypeptide mutants of *Escherichia coli*. *J Biol Chem*. 1990;265:19560-7.
- [22] Weiner JH, Cammack R, Cole ST, Condon C, Honore N, Lemire BD, et al. A mutant of *Escherichia coli* fumarate reductase decoupled from electron transport. *Proc Natl Acad Sci U S A*. 1986;83:2056-60.
- [23] Weiner JH, Dickie P. Fumarate reductase of *Escherichia coli*. Elucidation of the covalent-flavin component. *J Biol Chem*. 1979;254:8590-3.
- [24] Carlson MR, Zhang B, Fang Z, Mischel PS, Horvath S, Nelson SF. Gene connectivity, function, and sequence conservation: predictions from modular yeast co-expression networks. *BMC Genomics*. 2006;7:40.
- [25] Luo F, Yang Y, Zhong J, Gao H, Khan L, Thompson DK, et al. Constructing gene co-expression networks and predicting functions of unknown genes by random matrix theory. *BMC Bioinformatics*. 2007;8:299.
- [26] Costanzo M, Baryshnikova A, Bellay J, Kim Y, Spear ED, Sevier CS, et al. The genetic landscape of a cell. *Science*. 2010;327:425-31.

- [27] Hume DA, Summers KM, Raza S, Baillie JK, Freeman TC. Functional clustering and lineage markers: insights into cellular differentiation and gene function from large-scale microarray studies of purified primary cell populations. *Genomics*. 2010;95:328-38.
- [28] Salmon K, Hung SP, Mekjian K, Baldi P, Hatfield GW, Gunsalus RP. Global gene expression profiling in *Escherichia coli* K12. The effects of oxygen availability and FNR. *J Biol Chem*. 2003;278:29837-55.
- [29] Kang Y, Weber KD, Qiu Y, Kiley PJ, Blattner FR. Genome-wide expression analysis indicates that FNR of *Escherichia coli* K-12 regulates a large number of genes of unknown function. *J Bacteriol*. 2005;187:1135-60.
- [30] Munch R, Hiller K, Grote A, Scheer M, Klein J, Schobert M, et al. Virtual Footprint and PRODORIC: an integrative framework for regulon prediction in prokaryotes. *Bioinformatics*. 2005;21:4187-9.
- [31] Chakravarty A, Carlson JM, Khetani RS, Gross RH. A novel ensemble learning method for *de novo* computational identification of DNA binding sites. *BMC Bioinformatics*. 2007;8:249.
- [32] Studholme DJ, Dixon R. Domain architectures of sigma54-dependent transcriptional activators. *J Bacteriol*. 2003;185:1757-67.
- [33] Green J, Scott C, Guest JR. Functional versatility in the CRP-FNR superfamily of transcription factors: FNR and FLP. *Adv Microb Physiol*. 2001;44:1-34.
- [34] Lazazzera BA, Bates DM, Kiley PJ. The activity of the *Escherichia coli* transcription factor FNR is regulated by a change in oligomeric state. *Genes Dev*. 1993;7:1993-2005.
- [35] Chenault SS, Earhart CF. Organization of genes encoding membrane proteins of the *Escherichia coli* ferrienterobactin permease. *Mol Microbiol*. 1991;5:1405-13.
- [36] Lavrrar JL, Christoffersen CA, McIntosh MA. Fur-DNA interactions at the bidirectional *fepDGC-entS* promoter region in *Escherichia coli*. *J Mol Biol*. 2002;322:983-95.
- [37] Chen Z, Lewis KA, Shultzaberger RK, Lyakhov IG, Zheng M, Doan B, et al. Discovery of Fur binding site clusters in *Escherichia coli* by information theory models. *Nucleic Acids Res*. 2007;35:6762-77.
- [38] Messenger SL, Green J. FNR-mediated regulation of *hyp* expression in *Escherichia coli*. *FEMS Microbiol Lett*. 2003;228:81-6.
- [39] Tyson KL, Bell AI, Cole JA, Busby SJ. Definition of nitrite and nitrate response elements at the anaerobically inducible *Escherichia coli* nirB promoter: interactions between FNR and NarL. *Mol Microbiol*. 1993;7:151-7.
- [40] Babu M, Butland G, Pogoutse O, Li J, Greenblatt JF, Emili A. Sequential peptide affinity purification system for the systematic isolation and identification of protein complexes from *Escherichia coli*. *Methods Mol Biol*. 2009;564:373-400.

- [41] Grainger DC, Aiba H, Hurd D, Browning DF, Busby SJ. Transcription factor distribution in *Escherichia coli*: studies with FNR protein. *Nucleic Acids Res.* 2007;35:269-78.
- [42] Federowicz S, Kim D, Ebrahim A, Lerman J, Nagarajan H, Cho BK, et al. Determining the control circuitry of redox metabolism at the genome-scale. *PLoS genetics.* 2014;10:e1004264.
- [43] King T, Ferenci T. Divergent roles of RpoS in *Escherichia coli* under aerobic and anaerobic conditions. *FEMS Microbiol Lett.* 2005;244:323-7.
- [44] Tsai YC, Lapina MC, Bhushan S, Mueller-Cajar O. Identification and characterization of multiple rubisco activases in chemoautotrophic bacteria. *Nat Commun.* 2015;6:8883.
- [45] Datsenko KA, Wanner BL. One-step inactivation of chromosomal genes in *Escherichia coli* K-12 using PCR products. *Proc Natl Acad Sci U S A.* 2000;97:6640-5.
- [46] Miller JH. A short course in bacterial genetics: a laboratory manual and handbook for *Escherichia coli* and related bacteria. Plainview, NY: Cold Spring Harbor Laboratory Press; 1992.
- [47] Merlin C, Gardiner G, Durand S, Masters M. The *Escherichia coli* metD locus encodes an ABC transporter which includes Abc (MetN), YaeE (MetI), and YaeC (MetQ). *J Bacteriol.* 2002;184:5513-7.
- [48] Baba T, Ara T, Hasegawa M, Takai Y, Okumura Y, Baba M, et al. Construction of *Escherichia coli* K-12 in-frame, single-gene knockout mutants: the Keio collection. *Mol Syst Biol.* 2006;2:2006 0008.
- [49] Yamamoto N, Nakahigashi K, Nakamichi T, Yoshino M, Takai Y, Touda Y, et al. Update on the Keio collection of *Escherichia coli* single-gene deletion mutants. *Mol Syst Biol.* 2009;5:335.
- [50] Zeghouf M, Li J, Butland G, Borkowska A, Canadien V, Richards D, et al. Sequential Peptide Affinity (SPA) system for the identification of mammalian and bacterial protein complexes. *J Proteome Res.* 2004;3:463-8.
- [51] De Marco V, Stier G, Blandin S, de Marco A. The solubility and stability of recombinant proteins are increased by their fusion to NusA. *Biochem Biophys Res Commun.* 2004;322:766-71.
- [52] Faith JJ, Driscoll ME, Fusaro VA, Cosgrove EJ, Hayete B, Juhn FS, et al. Many Microbe Microarrays Database: uniformly normalized Affymetrix compendia with structured experimental metadata. *Nucleic Acids Res.* 2008;36:D866-70.
- [53] Irizarry RA, Hobbs B, Collin F, Beazer-Barclay YD, Antonellis KJ, Scherf U, et al. Exploration, normalization, and summaries of high density oligonucleotide array probe level data. *Biostatistics.* 2003;4:249-64.

- [54] Keseler IM, Collado-Vides J, Gama-Castro S, Ingraham J, Paley S, Paulsen IT, et al. EcoCyc: a comprehensive database resource for *Escherichia coli*. *Nucleic Acids Res.* 2005;33:D334-7.
- [55] Magrane M, UniProt C. UniProt Knowledgebase: a hub of integrated protein data. *Database (Oxford)*. 2011;2011:bar009.
- [56] Gama-Castro S, Salgado H, Peralta-Gil M, Santos-Zavaleta A, Muniz-Rascado L, Solano-Lira H, et al. RegulonDB version 7.0: transcriptional regulation of *Escherichia coli* K-12 integrated within genetic sensory response units (Gensor Units). *Nucleic Acids Res.* 2011;39:D98-105.
- [57] Zhang X, Bremer H. Control of the *Escherichia coli* *rrnB* P1 promoter strength by ppGpp. *J Biol Chem.* 1995;270:11181-9.
- [58] Savitzky A, Golay MJE. Smoothing + Differentiation of Data by Simplified Least Squares Procedures. *Anal Chem.* 1964;36:1627-&.
- [59] Micsonai A, Wien F, Kernya L, Lee YH, Goto Y, Refregiers M, et al. Accurate secondary structure prediction and fold recognition for circular dichroism spectroscopy. *Proc Natl Acad Sci U S A.* 2015;112:E3095-103.
- [60] Hayes D, Laue T, Philo J. Program Sednterp: sedimentation interpretation program. Alliance Protein Laboratories, Thousand Oaks, CA. 1995.
- [61] Kreuzer KN, Jongeneel CV. *Escherichia coli* phage T4 topoisomerase. *Methods Enzymol.* 1983;100:144-60.
- [62] Neidhardt FC, Bloch PL, Smith DF. Culture medium for enterobacteria. *J Bacteriol.* 1974;119:736-47.
- [63] Bilous PT, Weiner JH. Dimethyl sulfoxide reductase activity by anaerobically grown *Escherichia coli* HB101. *J Bacteriol.* 1985;162:1151-5.
- [64] Typas A, Becker G, Hengge R. The molecular basis of selective promoter activation by the sigmaS subunit of RNA polymerase. *Mol Microbiol.* 2007;63:1296-306.
- [65] Mendoza-Vargas A, Olvera L, Olvera M, Grande R, Vega-Alvarado L, Taboada B, et al. Genome-wide identification of transcription start sites, promoters and transcription factor binding sites in *E. coli*. *PloS one.* 2009;4:e7526.

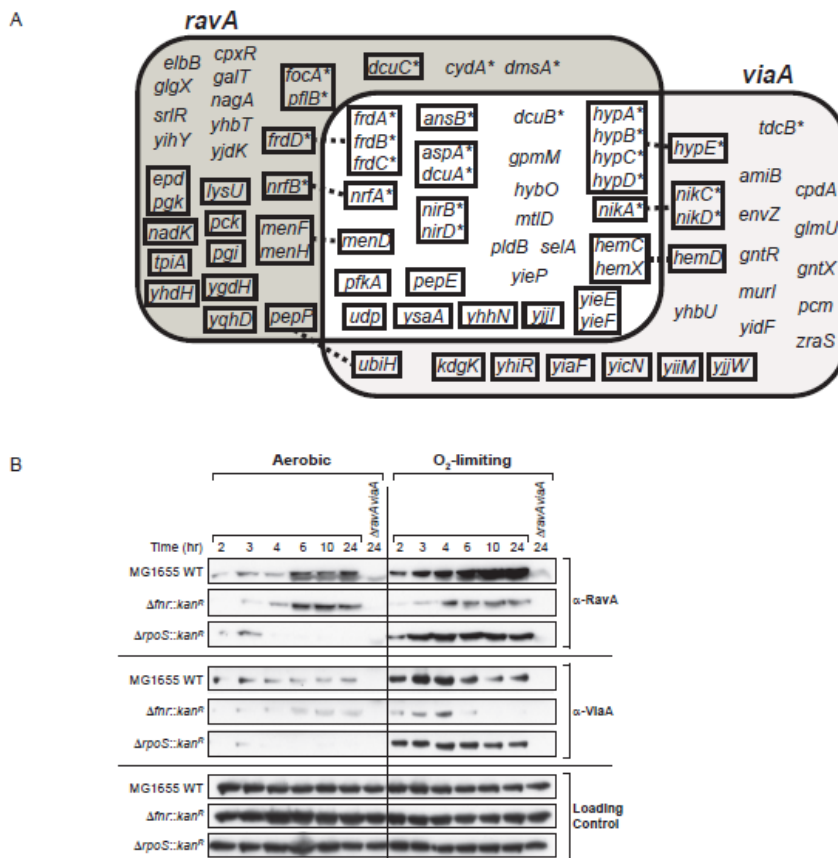


Figure 1

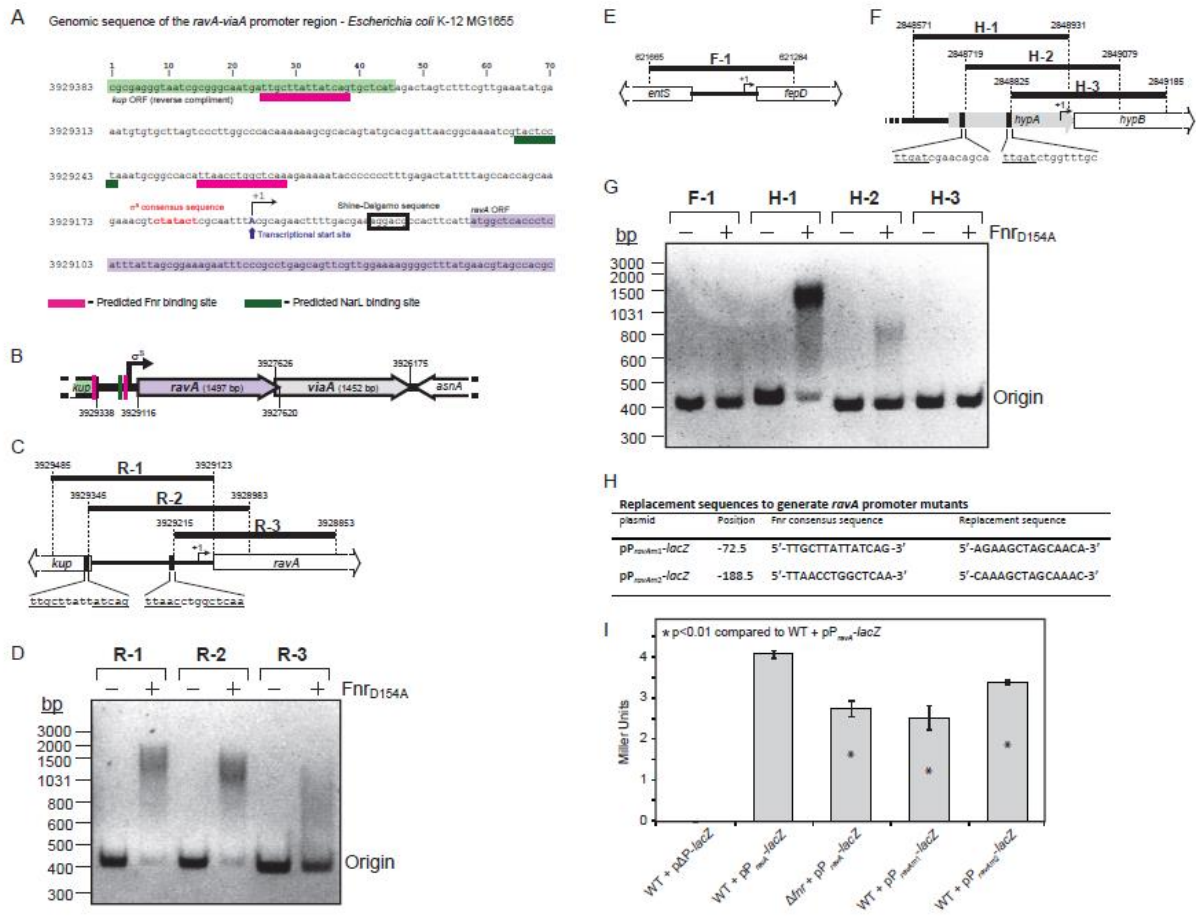


Figure 2

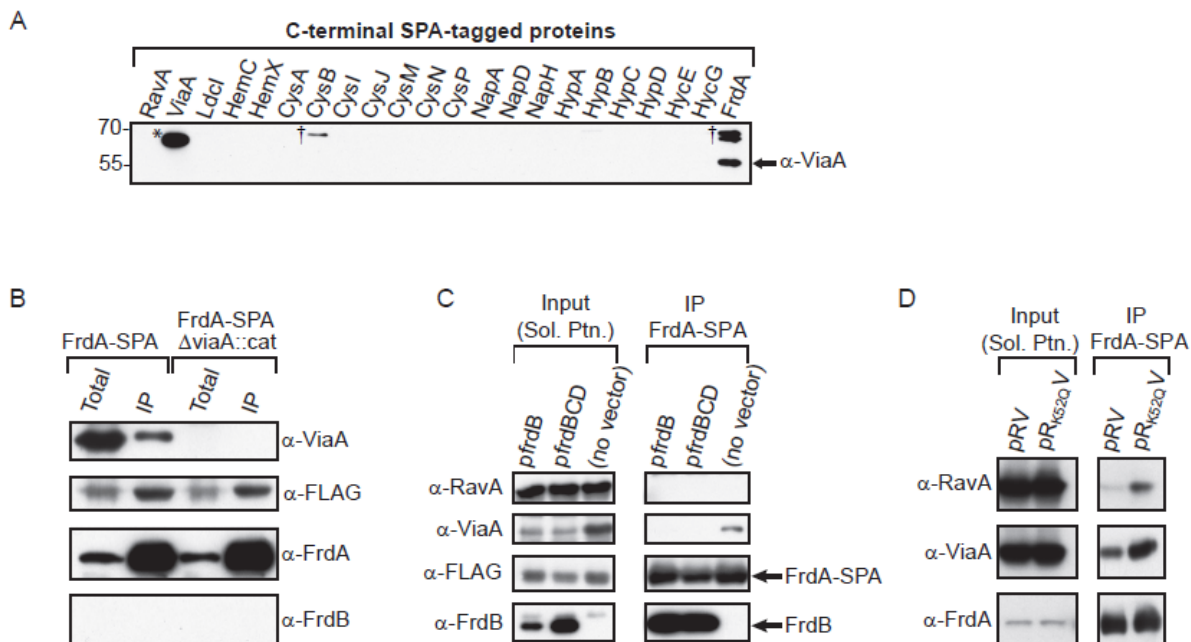


Figure 3

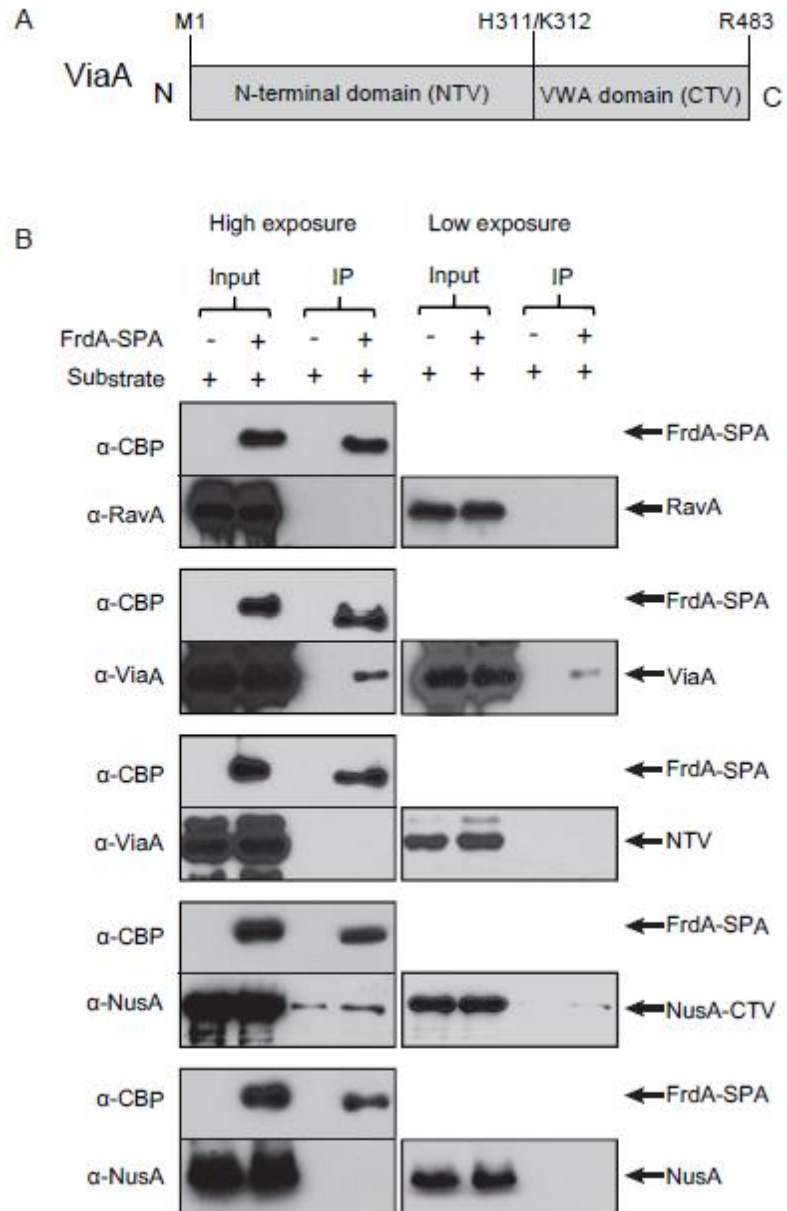


Figure 4

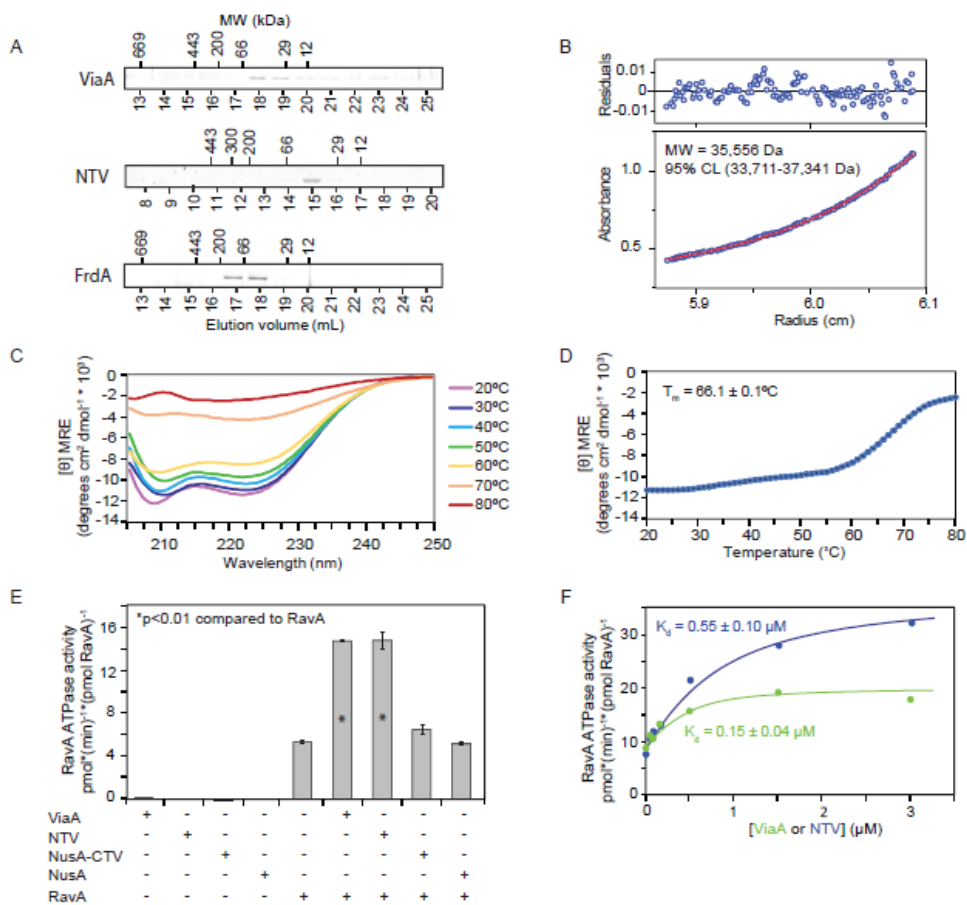


Figure 5

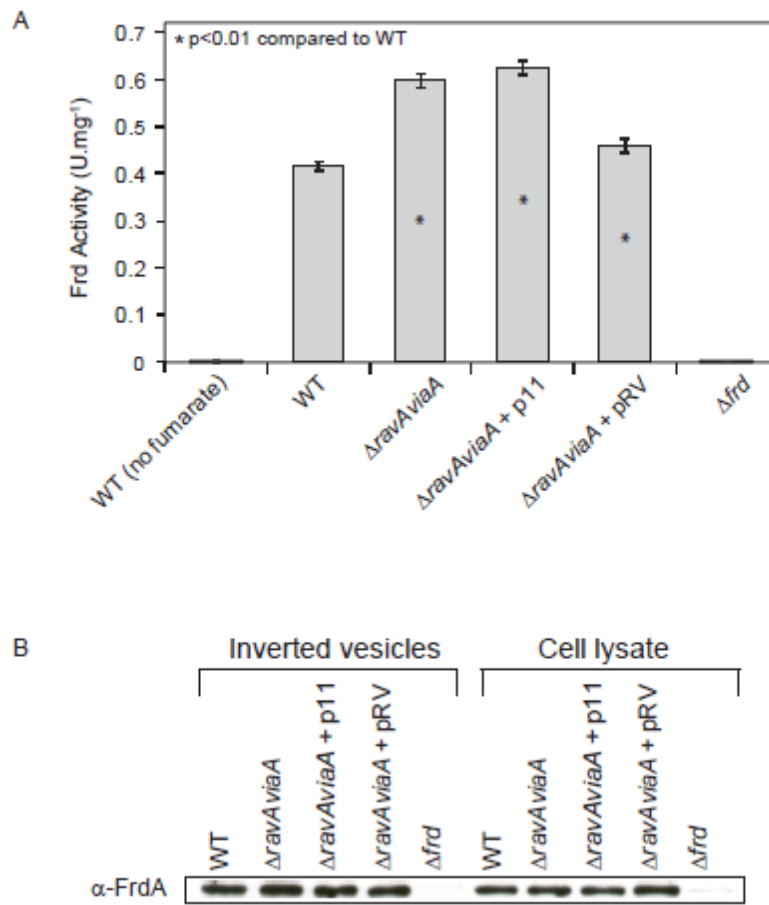


Figure 6

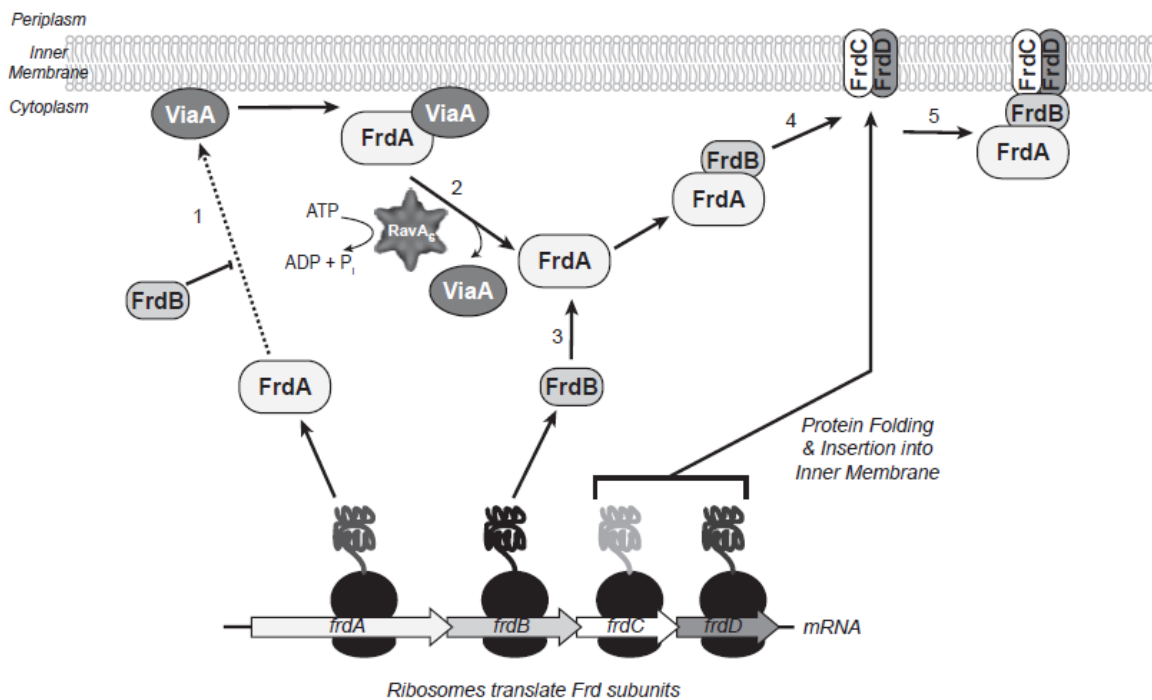


Figure 7

Table 1. Pearson correlation scores for *ravA*- and *viaA*-co-expressing genes and their functional annotations

The following list contains genes that meet the stringent cut-off (correlation score ≥ 0.5) and are considered to co-express with *ravA* and/or *viaA*. The Pearson correlation scores corresponding to each of these genes are provided on the right. The b numbers and functional descriptions (if available) are also provided as shown. The genes are divided into three categories, depending on whether they co-express with both *ravA* and *viaA* (Category I), with *ravA* only (Category II), or with *viaA* only (Category III). A Venn diagram of the data is given in Figure 1A.

Category I: Genes co-expressing with both *ravA* and *viaA*

Gene Name	b Number	Description	Correlation with <i>ravA</i>	Correlation with <i>viaA</i>
<i>ansB</i>	b2957	Asn metabolism	0.65051	0.60753
<i>aspA</i>	b4139	Asp metabolism	0.54194	0.57059
<i>dcuA</i>	b4138	C4-dicarboxylate transport	0.66535	0.54888
<i>dcuB</i>	b4123	C4-dicarboxylate transport	0.56817	0.51744
<i>frdA</i>	b4154	Anaerobic respiration; Fermentation	0.69038	0.63405
<i>frdB</i>	b4153	Anaerobic respiration; Fermentation	0.64379	0.60204
<i>frdC</i>	b4152	Anaerobic respiration; Fermentation	0.61917	0.5964
<i>gpmM</i>	b3612	Glycolysis	0.59776	0.52958
<i>hemC</i>	b3805	Hem biosynthesis	0.51487	0.50138
<i>hemX</i>	b3803	Porphyrin biosynthesis	0.5281	0.54115
<i>hybO</i>	b2997	Anaerobic respiration	0.62005	0.58672
<i>hypA</i>	b2726	Protein modification; Anaerobic respiration	0.64622	0.5954
<i>hypB</i>	b2727	Protein maturation	0.69607	0.62498
<i>hypC</i>	b2728	Protein maturation; Anaerobic respiration	0.67458	0.63329
<i>hypD</i>	b2729	Protein modification; Anaerobic respiration	0.65885	0.59676
<i>menD</i>	b2264	Menaquinone biosynthesis	0.54297	0.50761
<i>mtlD</i>	b3600	Carbohydrate catabolism	0.50802	0.56832
<i>nikA</i>	b3476	Ni ²⁺ transport	0.54464	0.55937
<i>nirB</i>	b3365	Anaerobic respiration; nitrate assimilation	0.57724	0.51632
<i>nirD</i>	b3366	Anaerobic respiration; nitrate assimilation	0.53498	0.51578
<i>nrfA</i>	b4070	Anaerobic respiration	0.53363	0.51896
<i>pepE</i>	b4021	Glycopeptide catabolism	0.65684	0.56658
<i>pfkA</i>	b3916	Glycolysis	0.56294	0.51026
<i>pldB</i>	b3825	Lipid biosynthesis	0.52289	0.59484
<i>selA</i>	b3591	Selenocysteine incorporation	0.69996	0.62336
<i>udp</i>	b3831	Nucleoside metabolism	0.50767	0.53799
<i>yhhN</i>	b3468		0.54876	0.5435
<i>yieE</i>	b3712		0.5822	0.53172
<i>yieF</i>	b3713	Xenobiotic metabolism	0.55289	0.55248
<i>yieP</i>	b3755	Transcription regulation	0.59788	0.57585
<i>yjiI</i>	b4380		0.70975	0.69532
<i>ysaA</i>	b3573	Electron transport chain	0.61717	0.56855

Category II: Genes co-expressing with *ravA* only

Gene Name	b Number	Description	Correlation with <i>ravA</i>
<i>cpxR</i>	b3912	DNA-binding response regulator in two-component regulatory system with CpxA	0.56566
<i>cydA</i>	b0733	cytochrome d terminal oxidase, subunit I	0.51738
<i>dcuC</i>	b0621	anaerobic C4-dicarboxylate transport	0.52104
<i>dmsA</i>	b0894	dimethyl sulfoxide reductase, anaerobic, subunit A	0.5548

<i>elbB</i>	b3209	isoprenoid biosynthesis protein with amidotransferase-like domain	0.50812
<i>epd</i>	b2927	D-erythrose 4-phosphate dehydrogenase	0.50287
<i>focA</i>	b0904	formate transporter	0.52822
<i>frdD</i>	b4151	fumarate reductase (anaerobic), membrane anchor subunit	0.50535
<i>galT</i>	b0758	galactose-1-phosphate uridylyltransferase	0.50055
<i>glgX</i>	b3431	glycogen debranching enzyme	0.52472
<i>lysU</i>	b4129	lysine tRNA synthetase, inducible	0.53954
<i>menF</i>	b2265	isochorismate synthase 2	0.52301
<i>nadK</i>	b2615	NAD kinase	0.54078
<i>nagA</i>	b0677	N-acetylglucosamine-6-phosphate deacetylase	0.55783
<i>nrfB</i>	b4071	nitrite reductase, formate-dependent, penta-heme cytochrome c	0.51511
<i>pck</i>	b3403	phosphoenolpyruvate carboxykinase	0.50262
<i>pepP</i>	b2908	proline aminopeptidase P II	0.5116
<i>pflB</i>	b0903	pyruvate formate lyase I (inactive)	0.52252
<i>pgi</i>	b4025	glucosephosphate isomerase	0.53519
<i>pgk</i>	b2926	phosphoglycerate kinase	0.53232
<i>srlR</i>	b2707	GutR glucitol repressor	0.58033
<i>tpiA</i>	b3919	triosephosphate isomerase	0.57139
<i>viaA</i>	b3745	VWA-containing protein associated with RavA	0.84586
<i>yfbB</i>	b2263	(1R,6R)-2-succinyl-6-hydroxy-2,4-cyclohexadiene-1-carboxylate synthase	0.50662
<i>ygdH</i>	b2795	hypothetical protein	0.5543
<i>yhbT</i>	b3157	predicted lipid carrier protein	0.52801
<i>yhdH</i>	b3253	predicted oxidoreductase, Zn-dependent and NAD(P)-binding	0.54479
<i>yihY</i>	b3886	predicted inner membrane protein	0.5313
<i>yjdK</i>	b4128	hypothetical protein	0.56851
<i>yqhD</i>	b3011	alcohol dehydrogenase, NAD(P)-dependent	0.55211

Category III: Genes co-expressing with *viaA* only

Gene Name	b Number	Description	Correlation with <i>viaA</i>
<i>amiB</i>	b4169	N-acetylmuramoyl-l-alanine amidase II	0.52138
<i>cpdA</i>	b3032	cyclic 3',5'-adenosine monophosphate phosphodiesterase	0.53408
<i>envZ</i>	b3404	sensory histidine kinase in two-component regulatory system with OmpR	0.53976
<i>glmU</i>	b3730	fused N-acetyl glucosamine-1-phosphate uridylyltransferase and glucosamine-1-phosphate acetyl transferase	0.52324
<i>gntR</i>	b3438	DNA-binding transcriptional repressor	0.5719
<i>gntX</i>	b3413	gluconate periplasmic binding protein with phosphoribosyltransferase domain, GNT I system	0.50584
<i>hemD</i>	b3804	uroporphyrinogen III synthase	0.50487
<i>hypE</i>	b2730	carbamoyl phosphate phosphatase, hydrogenase 3 maturation protein	0.51627
<i>kdgK</i>	b3526	2-keto-3-deoxygluconokinase	0.54256
<i>murI</i>	b3967	glutamate racemase	0.51627
<i>nikC</i>	b3478	nickel transporter subunit	0.52011
<i>nikD</i>	b3479	nickel transporter subunit	0.50367
<i>pcm</i>	b2743	L-isoaspartate protein carboxylmethyltransferase type II	0.53129
<i>ravA</i>	b3746	MoxR AAA+ ATPase interacting with LdcI	0.84586
<i>tdcB</i>	b3117	catabolic threonine dehydratase, PLP-dependent	0.51152
<i>ubiH</i>	b2907	2-octaprenyl-6-methoxyphenol hydroxylase, FAD/NAD(P)-binding	0.51134

<i>yhbU</i>	b3158	predicted peptidase, collagenase-like	0.54514
<i>yhiR</i>	b3499	Protein utilizing DNA as a carbon source	0.53345
<i>yiaF</i>	b3554	hypothetical protein	0.52386
<i>yicN</i>	b3663	hypothetical protein	0.62638
<i>yidF</i>	b3674	predicted DNA-binding transcriptional regulator	0.5513
<i>yiiM</i>	b3910	protein involved in base analog detoxification	0.53678
<i>yijW</i>	b4379	predicted pyruvate formate lyase activating enzyme	0.5497
<i>zraS</i>	b4003	sensory histidine kinase in two-component regulatory system with ZraR	0.54079

Table 2. List of bacterial strains, plasmids and primers

<i>Bacterial strains</i>	<i>Genotype</i>	<i>Reference</i>
MG1655 (WT)	F-, <i>rph-1</i> , λ -	[1]
MG1655 Δ <i>ravAviaA</i>	MG1655, Δ <i>ravAviaA</i>	This study
MG1655 Δ <i>fnr::kan^R</i>	MG1655, Δ <i>fnr::kan^R</i>	This study
MG1655 Δ <i>rpoS::kan^R</i>	MG1655, Δ <i>rpoS::kan^R</i>	This study
PK22	BL21(DE3), Δ <i>crp-bs990</i> , <i>rpsL</i> , Δ <i>fnr</i> , <i>zcy-3061::Tn10</i>	[2]
DY330 (WT)	W3110, Δ <i>lacU169</i> , <i>gal490</i> , <i>pgl</i> Δ 8 λ , [ρ]c1857 (<i>cro-bioA</i>)	[3]
DY330 RavA-SPA	DY330, <i>ravA-SPA::kan^R</i>	This study
DY330 ViaA-SPA	DY330, <i>viaA-SPA::kan^R</i>	This study
DY330 LdcI-SPA	DY330, <i>ldcI-SPA::kan^R</i>	This study
DY330 FrdA-SPA	DY330, <i>frdA-SPA::kan^R</i>	This study
DY330 FrdA-SPA	DY330, <i>frdA-SPA::kan^R</i> , Δ <i>viaA::cat</i> Δ <i>viaA::cat</i>	This study
DY330 HemC-SPA	DY330, <i>hemC-SPA::kan^R</i>	This study
DY330 HemX- SPA	DY330, <i>hemX-SPA::kan^R</i>	This study
DY330 CysA-SPA	DY330, <i>cysA-SPA::kan^R</i>	This study
DY330 CysB-SPA	DY330, <i>cysB-SPA::kan^R</i>	This study
DY330 CysI-SPA	DY330, <i>cysI-SPA::kan^R</i>	This study
DY330 CysJ-SPA	DY330, <i>cysJ-SPA::kan^R</i>	This study
DY330 CysM-SPA	DY330, <i>cysM-SPA::kan^R</i>	This study
DY330 CysN-SPA	DY330, <i>cysN-SPA::kan^R</i>	This study
DY330 CysP-SPA	DY330, <i>cysP-SPA::kan^R</i>	This study
DY330 NapA-SPA	DY330, <i>napA-SPA::kan^R</i>	This study

DY330 NapD-SPA	DY330, <i>napD-SPA::kan^R</i>	This study
DY330 NapH-SPA	DY330, <i>napH-SPA::kan^R</i>	This study
DY330 HypA-SPA	DY330, <i>hypA-SPA::kan^R</i>	This study
DY330 HypB-SPA	DY330, <i>hypB-SPA::kan^R</i>	This study
DY330 HypC-SPA	DY330, <i>hypC-SPA::kan^R</i>	This study
DY330 HypD-SPA	DY330, <i>hypD-SPA::kan^R</i>	This study
DY330 HycE-SPA	DY330, <i>hycE-SPA::kan^R</i>	This study
DY330 HycG-SPA	DY330, <i>hycG-SPA::kan^R</i>	This study
EDCM 367 (WT)	MG1655 Δ (P _{lac} - <i>lacZY</i>)	[4]
EDCM 367 Δ <i>fnr</i>	EDCM 367, Δ <i>fnr</i>	This study
BL21 Gold (DE3)	BL21 (DE3), pLysS(<i>T7p20 ori_{p15A}</i>)(Cm ^R) pLysS	Stratagene

<i>Plasmids</i>	<i>Description</i>	<i>Reference</i>
p11	Cloning vector derived from pET15b(+)	[5]
pRV	p11- <i>ravAp-ravA</i> <i>viaA</i> , for RavA and ViaA overexpression regulated by the native <i>ravA</i> promoter	[6]
pR _{K52Q} V	p11- <i>ravAp-ravA(K52Q)viaA</i> , for the overexpression of RavA Walker A mutant and wildtype ViaA regulated by the native <i>ravA</i> promoter	This study
pPK824	pET11a- <i>fnrD154A</i> , for IPTG-induced expression of the mutant FnrD154A	[2]
p11- <i>frdp</i>	p11- <i>frdp</i> ; <i>frd</i> promoter control for similar plasmids carrying genes encoding the subunits of fumarate reductase	This study
pfrdB	p11- <i>frdp-frdB</i> , for overexpressing FrdB regulated by the native <i>frd</i> promoter	This study
pfrdBCD	p11- <i>frdp-frdBCD</i> , for overexpressing FrdB, FrdC and FrdD regulated by the native <i>frd</i> promoter	This study
pETm-60	Cloning vector	[7]
pP _{<i>ravA</i>} - <i>lacZ</i>	pETm-60 (<i>ravAp-lacZ</i>) for β -galactosidase expression under native <i>ravA</i> promoter control	This study
pP _{<i>ravAm1</i>} - <i>lacZ</i>	pETm-60 (<i>ravAp^{fnr1}-lacZ</i>) β -galactosidase expression under control of <i>ravA</i> promoter mutant with replacement of the putative Fnr binding	This study

sequence, centered at -72.5 from transcription start site.

pP _{ravAm2} - <i>lacZ</i>	pETm-60 (<i>ravAp^{fmr2}-lacZ</i>) β -galactosidase expression under control of <i>ravA</i> promoter with replacement of the putative Fnr binding site situated at -188.5 from transcription start site.	This study
p Δ P- <i>lacZ</i>	pETm-60 vector backbone with β -galactosidase encoding <i>lacZ</i> gene but no promoters.	This study
pET3aTr	Cloning vector	[8]
pET3aTr FrdA-SPA	Plasmid for the T7 inducible expression of FrdA-SPA fusion protein	This study
pETm-60 ViaA	Plasmid for the T7 inducible expression of NusA-ViaA fusion protein	This study
p11-RavA	Plasmid for the T7 inducible expression of RavA protein	This study
p11-NTV	Plasmid for the T7 inducible expression of NTV construct	This study
pETm-60 CTV	Plasmid for the T7 inducible expression of NusA-CTV fusion protein	This study

Primer name	Primer sequence (5' to 3')
RavA K52Q F	CGCCAGGTATTGCCCAAAGTTTGATCGCC
RavA K52Q R	GGCGATCAAACCTTTGGGCAATACCTGGCG
FrdABCD BamHI F	GATTATTATTGGATCCGGCTGCCAGGATGC
frdp NheI R	CATTATTATTGCTAGCCCTCCAGATTGTTTTATCCCAC
FrdA NheI R	CATTATTATTGCTAGCTCAGCCATTCGCCTTCTCCTC
FrdB NheI R	CATTATTATTGCTAGCTTAGCGTGGTTTCAGGGTCG
FrdD NheI R	CATTATTATTGCTAGCTTAGATTGTAACGACACCAATCAGCGTG
FrdB NheI F	GATTATTATTGCTAGCATGGCTGAGATGAAAAACCTGAAAATTG
FrdB XbaI R	CATTATTATTTCTAGATTAGCGTGGTTTCAGGGTCG
FrdD XbaI R	CATTATTATTTCTAGATTAGATTGTAACGACACCAATCAGCGTG
FrdA BamHI F	ACTGGGATCCGTGCAAACCTTTCAAGCCG
SPA HindIII R	GTCTAAGCTTCTACTTGTCATCGTCATCC
ViaA NcoI F	CATCCCATGGGAATGCTAACGCTGGATACGC
ViaA BamHI R	GTCTGGATCCTTATCGCCGCCAGCGTCTG
NTV NdeI F	ATGCCATATGCTAACGCTGGATACG

NTV BamHI R	ATGGATCCATGTACCACCGGACGTTGC
CTV NcoI F	CATGCCATGGGA AAAGATTACGATGAACAGCC
ravAp NcoI F	ATTCCATGGCACGGCATCGCGTTCAAC
ravAp BamHI R	ATTGGATCCGTGGCGTCCTTTCGTCAAAAAG
LacZ BamHI F	ATTGGATCCATGACCATGATTACGGATTCACTG
LacZ NotI R	ATTATTGCGGCCGCGACATGGCCTGCCCGGTT
ravAp(fnr1) F	CAAAGCTAGCAAACAGAAAAATACCCCCCTTIG
ravAp(fnr1) R	GTTTGCTAGCTTTGTGTGGCCGCATTTAGGAGTAC
ravAp(fnr2) F	GATTGCTAGCAACATGCTCATAGACTAGTCTTTTCG
ravAp(fnr2) R	GATTGCTAGCTTCTTCATTGCCCGCGATTACC
ravApNarLm F	GATTGCTAGCAAAAATGCGGCCACATTAACC
ravApNarLm R	GATTGCTAGCCGATTTTGCCGTTAATCGTG

<i>Primer name for EMSA</i>	<i>Primer sequence (5' to 3')</i>	<i>Description</i>
ravAp NcoI F	ATTCCATGGCACGGCATCGCGTTCAAC	Forward primer for R-1
ravAp BamHI R	ATTGGATCCGTGGCGTCCTTTCGTCAAAAAG	Reverse primer for R-1
ravAp(fnr1-2+) NcoI F	ATTCCATGGTGCTCATAGACTAGTCTTTCGTTGAAATATGAAATG	Forward primer for R-2
ravAp(fnr1-2+) BamHI R	ATTGGATCCAGGAGGAACACACTTTCACCACTTAATG	Reverse primer for R-2
ravAp(fnr1-2-) NcoI F	ATTCCATGGAGAAAAATACCCCCCTTTGAGAC	Forward primer for R-3
ravAp(fnr1-2-) BamHI R	ATTGGATCCAATAGAAAGGGGACCAAAAACCTTCTTCCG	Reverse primer for R-3
fepDp NcoI F	ATTTATTCCATGGCATCATCTGGATCTGCACCG	Forward primer for F-1
fepDp BamHI R	ATTTATTGGATCCGGCCTCCAGCACTACGGAAGCGG	Reverse primer for F-1
hypBp NcoI F	ATTCCATGGCGACGTGTCATTTTCGACATCATCGAC	Forward primer for H-1

hypBp BamHI R	ATTGGATCCGACACTGTGGACAGCGGC	Reverse primer for H-1
hypBp(fnr1-2+) NcoI F	ATTCCATGGGGCCGCAAAACACGGCGCAAAAC	Forward primer for H-2
hypBp(fnr1-2+) BamHI R	ATTGGATCCAAACGCGGAATGAGGGTTATGTTTCATCACC	Reverse primer for H-2
hypBp(fnr1-2-) NcoI F	ATTCCATGGCGCGGCAGCGTGGCGGAAG	Forward primer for H-3
hypBp(fnr1-2-) BamHI R	ATTGGATCCAATGCAGGTCGCCTTCTTCAGTCTGG	Reverse primer for H-3

cat = chloramphenicol acetyltransferase gene; confers resistance to chloramphenicol.

kan^R = kanamycin resistance gene

References

- [1] Guyer MS, Reed RR, Steitz JA, Low KB. Identification of a sex-factor-affinity site in *E. coli* as gamma delta. *Cold Spring Harb Symp Quant Biol.* 1981;45 Pt 1:135-40.
- [2] Lazazzera BA, Bates DM, Kiley PJ. The activity of the *Escherichia coli* transcription factor FNR is regulated by a change in oligomeric state. *Genes Dev.* 1993;7:1993-2005.
- [3] Yu D, Ellis HM, Lee EC, Jenkins NA, Copeland NG, Court DL. An efficient recombination system for chromosome engineering in *Escherichia coli*. *Proc Natl Acad Sci U S A.* 2000;97:5978-83.
- [4] Merlin C, Gardiner G, Durand S, Masters M. The *Escherichia coli* metD locus encodes an ABC transporter which includes Abc (MetN), YaeE (MetI), and YaeC (MetQ). *J Bacteriol.* 2002;184:5513-7.
- [5] Zhang RG, Skarina T, Katz JE, Beasley S, Khachatryan A, Vyas S, et al. Structure of *Thermotoga maritima* stationary phase survival protein SurE: a novel acid phosphatase. *Structure.* 2001;9:1095-106.
- [6] Snider J, Gutsche I, Lin M, Baby S, Cox B, Butland G, et al. Formation of a distinctive complex between the inducible bacterial lysine decarboxylase and a novel AAA+ ATPase. *J Biol Chem.* 2006;281:1532-46.
- [7] De Marco V, Stier G, Blandin S, de Marco A. The solubility and stability of recombinant proteins are increased by their fusion to NusA. *Biochem Biophys Res Commun.* 2004;322:766-71.
- [8] Tan S, Kern RC, Selleck W. The pST44 polycistronic expression system for producing protein complexes in *Escherichia coli*. *Protein Expr Purif.* 2005;40:385-95.

